UNIVERSITY OF SPLIT

FACULTY OF ELECTRICAL ENGINEERING, MECHANICAL ENGINEERING AND NAVAL ARCHITECTURE

DOCTORAL STUDIES IN MECHANICAL ENGINEERING

QUALIFYING EXAM

EFFICIENT NUMERICAL METHODS FOR MULTIPHASE FLOWS INTERACTING WITH STRUCTURES

MANIGANDAN PANEER

Split, December 2024

Contents

List of Figures

List of Tables

1 Introduction

Multiphase flow involves the simultaneous movement of different phases, such as liquids, gases, and solids, or immiscible fluids within a shared system. This phenomenon is fundamental and has significant implications across various industries and scientific fields. The dynamics of multiphase flows can be observed in many real-world applications, including oil and gas extraction, chemical processing, environmental science, nuclear reactor cooling, and biomedical engineering. The behavior of these flows often determines the efficiency, safety, and overall success of the processes involved, making it essential to understand and accurately model their underlying mechanisms. The distinct physical properties of each phase—such as density, viscosity, and compressibility—add complexity to multiphase flow modeling, especially as these phases interact with one another at their interfaces. The evolution of these interfaces is influenced by factors like surface tension, buoyancy forces, shear stresses, and other interfacial phenomena. These interactions can result in intricate behaviors, including droplet formation, bubble breakup, and particle aggregation. As a result of these complexities, multiphase flows can exhibit a wide range of behaviors, from stable stratified flows to highly chaotic and turbulent regimes. Therefore, effectively modeling multiphase flows is not only a significant scientific challenge, but it is also crucial for optimizing industrial applications, ensuring environmental safety, and advancing scientific research. The diversity of flow regimes in gas-liquid systems is illustrated in Figure 1.1 , which shows the transition between different flow types as liquid and gas velocities vary. Each regime represents a unique arrangement and interaction of the phases, highlighting the complexity and richness of multiphase flow behavior.

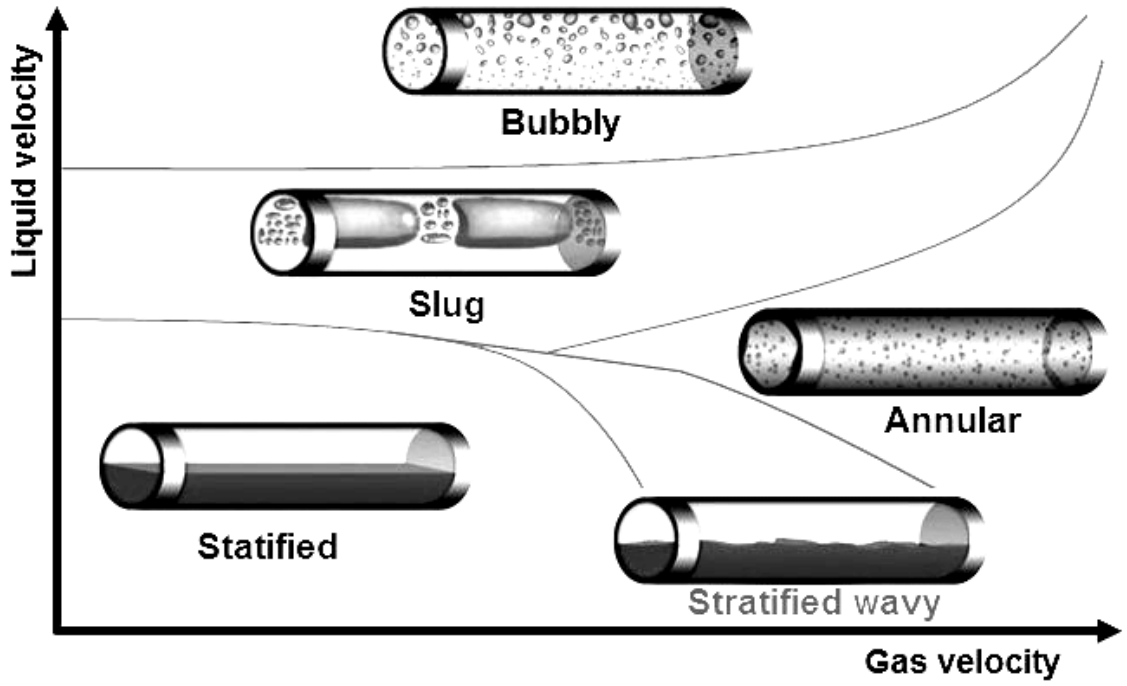

Figure 1.1: Diversity of flow regimes in gas-liquid systems

One of the unique challenges in modeling multiphase flow lies in the diverse range of flow regimes that can arise, depending on the relative velocities, properties, and orienta-

tions of the phases involved. In gas-liquid flows, for instance, these regimes include bubbly, slug, annular, stratified, and stratified wavy flows, each with distinct characteristics. Bubbly flow features dispersed gas bubbles within a continuous liquid phase, commonly seen in low-velocity gas streams. As gas velocity increases, these bubbles can coalesce to form larger gas slugs separated by liquid segments, leading to the slug flow regime. In annular flow, typically observed at higher gas velocities, a continuous gas core is surrounded by a thin liquid film. Stratified flow is characterized by a separated, layered arrangement of gas and liquid phases, while stratified wavy flow occurs when surface waves form at the interface due to higher relative velocities between the phases. These regimes are not only visually distinctive but also impact pressure drop, flow stability, and heat and mass transfer rates, which are critical factors in engineering design and operation.

In computational fluid dynamics (CFD), modeling multiphase flow is crucial for engineers and scientists who seek to accurately simulate complex systems. Traditional single-phase models often fall short in capturing the intricate interactions at phase boundaries and the unique phenomena associated with multiphase systems. To effectively simulate multiphase flows, specialized modeling techniques are necessary. These techniques must accommodate the distinct characteristics of each phase, account for interactions between phases, and manage the presence of phase interfaces. Recent research in this field has focused on developing robust, flexible, and computationally efficient multiphase flow models that cater to the diverse needs of various applications, ranging from large-scale industrial processes to microscale biological environments.

Key application areas in multiphase that includes precision spraying in industries like printing and electronics, where controlling droplet breakup and deposition patterns is essential. In paint atomization, high-frequency ultrasonic waves are used to break up the liquid, enabling fine control over droplet size and distribution. In underwater and ocean engineering, meshless methods excel in simulating wave interactions with floating bodies, sloshing, wave breaking, and other violent water-air interfaces. For sediment transport and oil spill simulations, capturing multiphase dynamics in irregularly shaped domains. Additionally, phase change phenomena such as boiling and condensation, supporting applications in cooling systems for microelectronics and thermal management in energy storage. In metal casting and additive manufacturing, the solver simulates complex processes involving fluid filling, droplet deposition, surface tension, and thermal effects.

One of the primary challenges in multiphase flow modeling is the accurate representation of phase interfaces. Capturing the movement, deformation, and interaction of phase boundaries is critical for accurately predicting multiphase flow behavior. Traditional grid-based methods often struggle to maintain sharp and stable interfaces, especially in systems with high-density and high-viscosity contrasts. Methods like the Level Set and Volume of Fluid techniques are commonly used for interface tracking, but they require complex algorithms to maintain numerical stability and prevent interface smearing. In addition to interface dynamics, surface tension forces play a significant role in multiphase flows, particularly in microscale systems where interfacial forces dominate over inertial forces. Surface tension affects behaviors such as droplet coalescence, breakup, and spreading, which are critical in applications like inkjet printing, microfluidics, and fuel injection. Accurate modeling of surface tension is challenging due to its highly localized nature, requiring precise algorithms and fine spatial resolution to capture its effects. Dynamic contact angles, which describe the interaction between fluid phases and solid surfaces, add another layer of complexity to multiphase flow modeling. These angles vary with flow conditions, influencing capillary-driven flows and the wettability of surfaces.

To address these challenges, recent advancements in computational methods and hardware have enabled the development of more robust and efficient multiphase flow models. GPU-accelerated solvers, for instance, offer significant computational speed-ups, making it feasible to simulate high-resolution, large-scale multiphase flows. In this work, we aim to develop a multiphase flow solver optimized for a range of complex applications, leveraging meshless methods for flexibility and precision in dynamic, high-deformation scenarios. Multiphase flows are crucial in various fields, from industrial processes to environmental and biomedical applications, etc. Our solver will model intricate phenomena such as droplet formation, phase change, dynamic contact angle, surface tension, fluid interaction and atomization supporting applications that demand accuracy in highly irregular or deforming domains.

Meshless methods provide a robust framework for simulating a wide range of multiphase flow applications with high accuracy and adaptability. They excel in applications such as oil extraction and transport, hydraulic fracturing, fuel cells, where they effectively model phenomena such as bubble dynamics, surface tension, and phase separation. Particularly suited for processes like hydrogen generation by accurately capturing bubble dynamics and phase interfaces, storage and mobility of hydrogen, oil spilling in marine environments, thermocapillary migration processes ensures precise heat transfer and controlled fluid migration and spray coating or painting on automotive and aircraft surfaces. In dip coating, where objects are dipped into a liquid to coat them, surface tension, fluid deformation, and contact angle dynamics are essential to control coating thickness and uniformity. This application is significant in industries such as automotive, electronics, and consumer goods. Dip deformation analysis is one of the important applications in automotive paint shop process which is connected with dip coating where multiphase flow with FSI is involved. Complex physical processes are involved in gearbox oil distribution simulation, e.g. violent multiphase flow, high-speed fluid structure interaction. Surface tension and ultrasonic sound-driven fluid injection in space and micro gravity application. The benefit of biofouling resistance comes from their capacity to manage fluid-solid interactions and dynamic boundary conditions. Multiphase flow with surface tension and dynamic contact angle play curial roles in many other applications like Digital micro fluids, Emulsion, Electro hydro-dynamics and etc,.

This paper is organized as follows: Section 2 presents the theoretical background, covering the governing equations, numerical methods, and key concepts such as surface tension, dynamic contact angle, and fluid-structure interaction (FSI). Section 3 provides a detailed literature review, discussing relevant studies on Lagrangian Differencing Dynamics (LDD), multiphase modeling, surface tension, dynamic contact angles, and FSI. Section 4 outlines the conclusion and future work, summarizing the scope of this study and proposing directions for future research.

2 Theoretical Background

2.1 Governing Equations

The Navier-Stokes equations governing incompressible fluids are expressed as follows:

$$\nabla \cdot \mathbf{u} = 0 \tag{2.1}$$

$$\frac{D\mathbf{u}}{Dt} = -\frac{1}{\rho}\nabla p + \nu\nabla^2\mathbf{u} + \mathbf{g} + \frac{1}{\rho}\mathbf{F}_s \tag{2.2}$$

In these equations,

- D/Dt is a material derivative, also known as the convective or substantial derivative
- $\mathbf{u}$ represents the velocity field
- ρ is the fluid density
- p denotes the pressure
- ν is the kinematic viscosity
- $\mathbf{g}$ stands for acceleration due to gravity and
- $\mathbf{F}_s$ signifies the force due to surface tension per unit volume.

The continuity equation $\nabla \cdot \mathbf{u} = 0$ ensures the incompressibility of the fluid, indicating that there are no sources or sinks within the fluid. The Momentum Equation (2.2) is based on the Lagrangian perspective, accounts for pressure gradients, viscous diffusion, gravitational forces, and surface tension forces. $\frac{D\mathbf{u}}{Dt}$ describe how the velocity of a fluid particle changes over time. For a velocity field $\mathbf{u}$, the material derivative is:

$$\frac{D\mathbf{u}}{Dt} = \frac{\partial \mathbf{u}}{\partial t} + \mathbf{u} \cdot \nabla \mathbf{u} \tag{2.3}$$

Where,

- $\partial\mathbf{u}/\partial t$ is the local acceleration and
- $\mathbf{u} \cdot \nabla\mathbf{u}$ is the convective acceleration.

Together, it describe the total acceleration of a fluid particle as it moves through the velocity field in the Lagrangian context. Solving the Navier-Stokes Equation (2.2) for incompressible flow involves determining both the pressure and velocity fields within a discretized computational domain. The pressure field is typically computed using the Pressure Poisson Equation (PPE) as below:

$$\nabla \cdot \left(\frac{\nabla p}{\rho}\right) = -\nabla \cdot D\mathbf{u}/Dt \tag{2.4}$$

The velocity field is typically computed as below:

$$\frac{D\mathbf{u}}{Dt} = -\frac{1}{\rho}\nabla p + \nu\nabla^2\mathbf{u} + \mathbf{g} + \frac{1}{\rho}\mathbf{F}_s \tag{2.5}$$

2.2 Numerical Methods

2.2.1 One Equation Approach

The one equation approach models multiphase flows by treating the entire domain as a single fluid, solving a single set of Navier-Stokes Equations (2.2). The differences in density and viscosity across phases are incorporated through fluid properties that vary spatially, defined as functions of a scalar field (e.g., volume fraction) [1, 2, 3, 4, 5]. Interface effects like surface tension are included by adding terms in the momentum equations to account for interfacial forces. This approach avoids explicitly tracking the interface, making it computationally efficient for complex flows. It can capture the behavior of interfaces in situations where phases do not separate sharply. Diffuse interfaces can arise, leading to a loss of sharpness in representing phase boundaries, especially for high-density ratio flows. Surface tension effects can be challenging to model accurately without a fine grid resolution in gird based methods. However, this can be easily adapted for the Lagrangian methods [6, 7]. Representation of the domain to solve the NS is shown in Figure 2.1

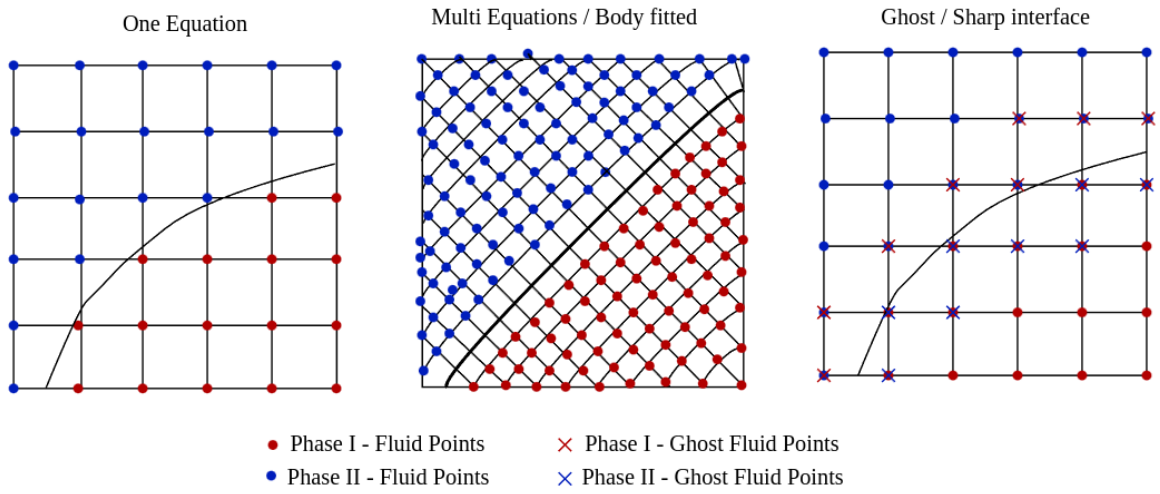

Figure 2.1: Representation of the domain to solve the NS for Multiphase flow. One equation Method (Left), Separate Equation for each phase is called Multi Equation (center), Ghost or sharp interface using ghost particles

2.2.2 Multi Equation Approach

For each phase, separate Navier-Stokes Equations (2.2) are solved, and conditions at the interface are applied to maintain continuity between two phases as below:

$$[\mathbf{u}_1 - \mathbf{u}_2] = 0 \quad \text{at the interface.} \tag{2.6}$$

Where,

- $\mathbf{u}_1$ is phase one velocity
- $\mathbf{u}_2$ is phase two velocity

It is best suited for cases where interfaces experience mild deformation. This method captures sharp interfaces precisely, providing high accuracy in phase boundary representation. Interface dynamics, including surface tension and phase changes, can be directly applied with continuity and boundary conditions [8, 9, 10, 11]. In Eulerian-based methods, It is achieved using body grid methods as shown in Figure 2.1

2.2.3 Ghost Fluid Method or Sharp Interface Methods

Sharp-interface methods, such as the Ghost Fluid Method (GFM), represent the interface between phases on a structured grid and use "ghost nodes" to capture discontinuities across the interface in the Eulerian method. These ghost nodes allow the method to interpolate values across the interface, avoiding the need for re-meshing while retaining a sharp interface. In Lagrangian methods, ghost particles are created by projection with respect to interface and compact radius. These methods solve the Navier-Stokes Equations (2.2) separately in each phase but include ghost nodes as shown in Figure 2.1, across the interface to handle discontinuities with ghost node values enforcing jump conditions [12, 13, 14, 15, 16, 17].

$$\left[\rho \frac{\partial \mathbf{u}}{\partial t}\right]_{\text{across interface}} = -\nabla p + \text{surface tension terms}, \tag{2.7}$$

2.3 Classification of Multiphase Modeling Techniques

Multiphase flow modeling encompasses various approaches, each tailored to specific applications and physical phenomena. The classification of these techniques can be broadly categorized into three primary groups: Molecular Modeling, Macroscopic Modeling, and Mesoscopic Modeling. Each category employs different methodologies and computational strategies to capture the complexities of multiphase interactions. Figure 2.2 presents a multiscale approach for modeling fluids across different time and length scales. At the smallest, quantum scale, atomic-level interactions are studied, focusing on electronic configurations. Moving up, the molecular scale models individual molecules and their dynamics, while the mesoscale groups collections of molecules, often using simplified methods to capture collective behavior like diffusion. At the largest, continuum scale, fluid properties are represented as averaged quantities (e.g., density, viscosity, and thermal conductivity), allowing for efficient modeling of large-scale fluid behavior. This framework enables selecting appropriate modeling techniques based on the scale of interest. Complete overview of multiphase modelling is shown in Figure 2.3

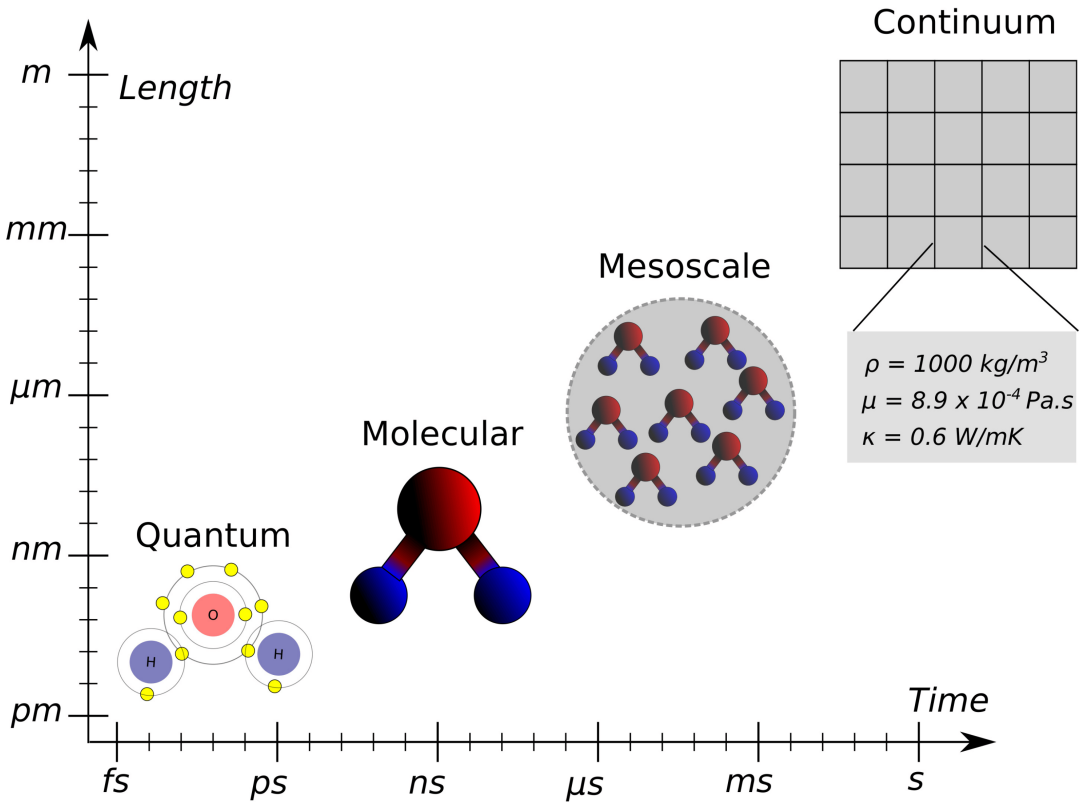

Figure 2.2: Multiscale Modeling Framework for Fluid Systems [18]

2.3.1 Molecular Modeling

Molecular modeling techniques focus on the fundamental interactions between molecules and are particularly useful for understanding phenomena at the nanoscale. This helps in understanding processes like diffusion, wetting, and nanoscale fluid behavior in pores.

Molecular Dynamics (MD): This method simulates the physical movements of atoms and molecules over time, providing insights into the properties of materials and interactions at the molecular level. However, MD is computationally intensive and not suitable for large-scale systems.

2.3.2 Mesoscopic Modeling

Mesoscopic modeling bridges the gap between molecular and macroscopic approaches, capturing essential features of multiphase flows without resorting to molecular details.

Dissipative Particle Dynamics (DPD): Describe DPD as a particle-based simulation technique that models interactions in a way that incorporates some macroscopic properties, allowing for the simulation of complex fluid behavior without resolving every molecular detail. DPD is useful for simulating soft matter and complex fluids. It is commonly applied in polymer science and biological simulations.

Lattice Boltzmann Method (LBM): A numerical approach based on kinetic theory that simulates fluid dynamics at the mesoscopic scale, effectively capturing complex boundary conditions and interface dynamics. LBM is widely used in porous media, multiphase interactions, and microfluidics

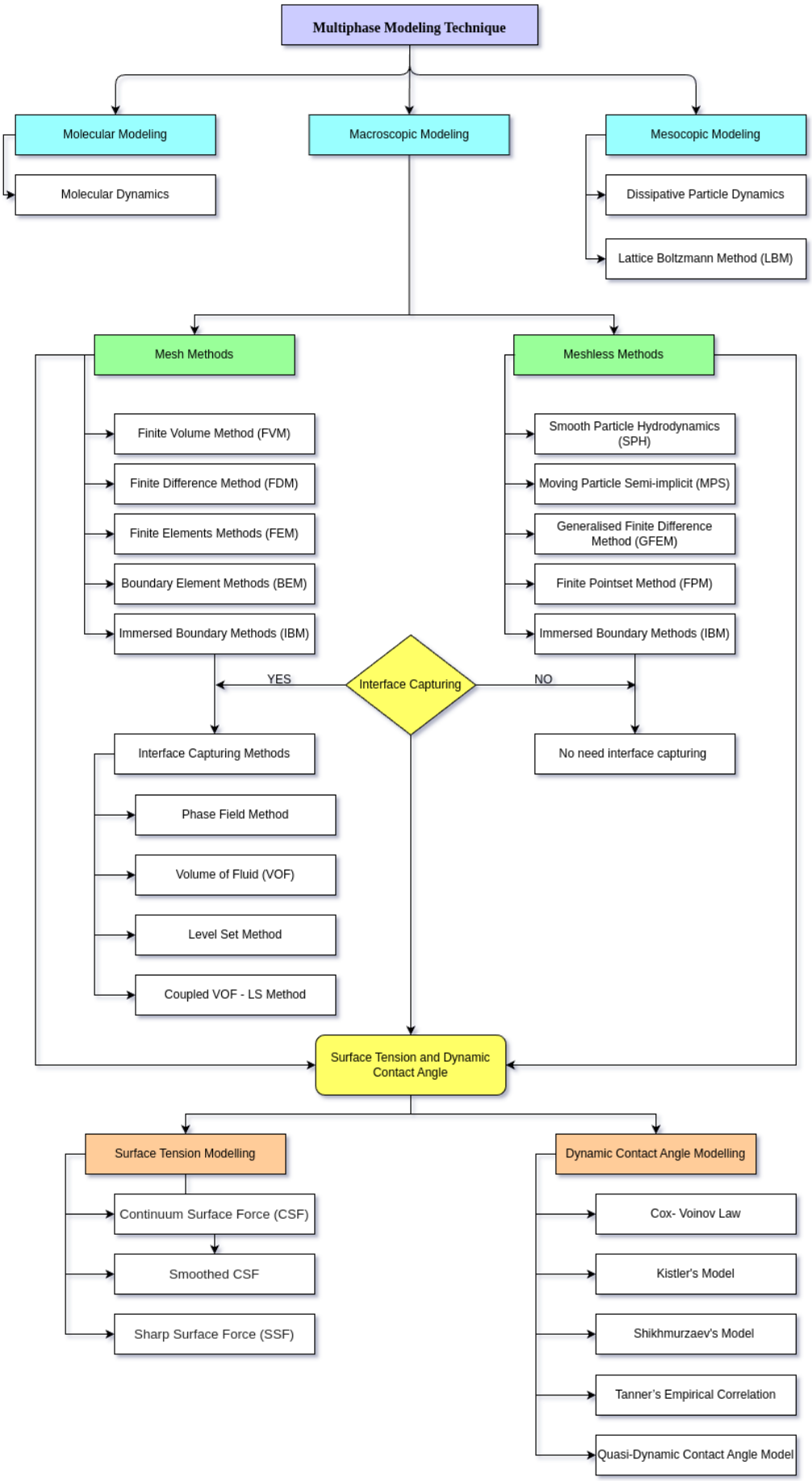

Figure 2.3: A detailed overview of Multiphase Modelling and Methods

2.3.3 Macroscopic Modeling

Macroscopic approach, which treats multiphase flows as continuous fields governed by partial differential equations. These models work at scales where continuum assumptions hold, allowing the phases to be treated as continuous, interpenetrating media. Macroscopic models are used extensively in industrial and environmental simulations, where large-scale flows and bulk properties are more important than individual particle interactions. It is widely classified as Mesh methods and Meshless methods.

Mesh Methods: Mesh or Grid based methods are numerical techniques employed to solve Partial Differential Equations (PDEs) by discretizing the continuous domain into a grid or mesh of points or cells as shown in Figure 2.4 . This discretization facilitates the approximation of continuous variables at specific locations, transforming the governing equations into a set of algebraic equations that can be solved numerically. By utilizing appropriate numerical schemes, the derivatives in the equations are estimated based on the values of neighboring grid points. These methods are versatile and adaptable, making them suitable for a wide array of applications in fluid dynamics, heat transfer, and structural analysis. Accurate specification of boundary and initial conditions is critical, as these significantly influence the solution. Overall, grid-based methods provide a systematic and efficient approach to analyzing complex physical phenomena across various scientific and engineering fields.

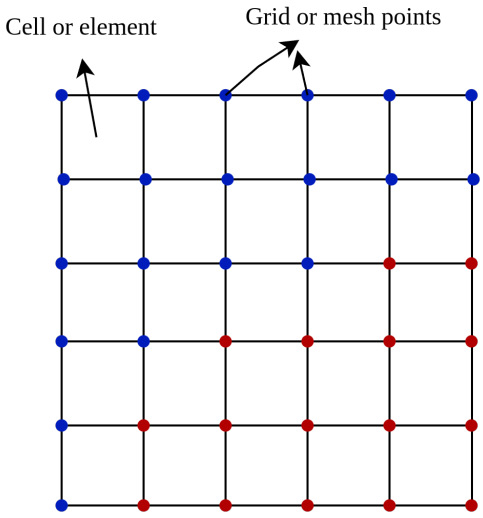

Figure 2.4: Representation of domain with mesh or grid for the mesh-based method

Finite Volume Method (FVM): The Finite Volume Method (FVM) is a robust numerical technique widely used to approximate solutions to partial differential equations, particularly in computational fluid dynamics (CFD) and heat transfer problems. This method divides the spatial domain of interest into small, discrete control volumes, each centered around a grid point. Within each control volume, integral conservation laws are applied for fundamental quantities such as mass, momentum, and energy. This framework ensures that the flux of a conserved quantity across the boundaries of each control volume is balanced, thereby upholding the physical principles of conservation throughout the simulation. In FVM, differential equations are transformed into algebraic equations by integrating over each control volume, simplifying complex partial differential equa-

tions that can then be solved iteratively. The adaptability of FVM allows it to manage irregular, non-uniform meshes and boundary conditions, which often arise in real-world applications. Its conservative nature makes it particularly effective for simulating flows with high accuracy across boundaries, even in complex geometries. The combination of flexibility, accuracy, and adherence to conservation principles positions the FVM as a preferred choice in engineering and scientific applications, where precise modeling of fluid flow, thermal transfer, and other transport phenomena is essential.

Finite Difference Method (FDM): The Finite Difference Method (FDM) is a numerical technique utilized to solve differential equations by approximating them with difference equations. This method is particularly beneficial for analyzing problems in computational fluid dynamics, heat conduction, and other domains governed by partial differential equations. FDM operates by discretizing the continuous domain into a grid, where derivatives are substituted with finite differences, enabling the transformation of differential equations into algebraic equations. In FDM, continuous variables are represented at discrete grid points, and the derivatives at these points are approximated using Taylor series expansions or simple difference formulas. For example, the first derivative can be approximated by the forward or backward difference, while higher-order derivatives may be represented using central differences. This results in a system of equations that can be solved iteratively or directly, contingent on the problem's complexity. One of the primary advantages of FDM is it's straightforward implementation and ease of use, especially for problems defined on structured grids. However, challenges may arise when dealing with complex geometries and irregular domains, where maintaining accuracy can be difficult. Despite these limitations, FDM remains a widely adopted approach due to its effectiveness in addressing time-dependent problems, offering good accuracy for smooth solutions, and providing a clear framework for both steady-state and transient analyses. It's versatility and relative simplicity render it a valuable tool in engineering and scientific research for modeling various physical phenomena.

Finite Element Method (FEM): The Finite Element Method (FEM) is a powerful numerical technique extensively employed in computational fluid dynamics (CFD) for solving complex partial differential equations that characterize fluid flow, heat transfer, and other physical phenomena. Unlike methods that utilize structured grids, FEM divides the computational domain into a mesh of small, simple shapes called elements, which can take various geometries (e.g., triangles or quadrilaterals in two dimensions, or tetrahedra or hexahedra in three dimensions). This flexibility enables FEM to effectively tackle complex geometries and boundary conditions frequently encountered in engineering applications. In FEM, governing differential equations are transformed into a weak formulation through the application of variational principles. Each element is assigned a set of shape functions that approximate the solution within that element. By integrating the governing equations over each element and applying the relevant boundary conditions, a system of algebraic equations is derived. These equations are then assembled into a global system representing the entire computational domain. The solution is obtained using numerical techniques, such as the Newton-Raphson method or iterative solvers, to resolve the resulting system of equations. A significant advantage of FEM in CFD is, it's capability to accurately model complex flow phenomena, including turbulence, phase interactions, and fluid-structure interactions. The method's adaptability to varying mesh densities allows for localized refinement, where a greater number of elements are utilized in regions with high gradients or complexity, thereby enhancing solution accuracy. Moreover, FEM is particularly well-suited for problems involving nonlinear behavior and

transient dynamics, making it a popular choice for simulating real-world fluid dynamics scenarios in fields such as aerospace, automotive, and biomedical engineering. It's robustness, flexibility, and accuracy position the FEM as a critical tool in the analysis and design of fluid systems.

Boundary Element Method (BEM): The Boundary Element Method (BEM) is a numerical technique employed to solve partial differential equations relevant to various engineering and physical applications, especially in fluid dynamics, heat transfer, and structural analysis. Unlike traditional methods that require full discretization of the entire volume of the domain, BEM focuses on the boundaries of the domain, significantly reducing the problem's dimensionality. This approach proves particularly efficient for problems involving infinite or semi-infinite domains, such as potential flow around objects or heat conduction in semi-infinite media. In BEM, the governing equations are reformulated in terms of boundary integrals, utilizing the boundary conditions of the problem to express the solution. The domain is divided into boundary elements, with the unknowns typically represented by interpolating functions over these boundaries. By applying integral equations derived from the governing differential equations, a system of equations is generated that correlates the unknown boundary values to the known boundary conditions. Solving this system yields the values at the boundaries, from which the solution in the entire domain can be reconstructed. A primary advantage of BEM is its capacity to accurately model problems with complex geometries and boundary conditions without requiring a dense mesh throughout the entire domain. Consequently, this results in fewer degrees of freedom compared to volume-based methods like FEM or FVM, thereby reducing computational cost and time. BEM is particularly effective for steady-state problems and those involving linear differential equations. However, it may be less efficient for nonlinear problems and may necessitate special handling for non-homogeneous boundary conditions.

Immersed Boundary Method (IBM): The Immersed Boundary Method (IBM) is a numerical technique utilized to simulate fluid flow in the presence of complex, moving geometries. This method is particularly advantageous in CFD for scenarios involving fluid-structure interactions, such as biological systems (e.g., blood flow around heart valves or fish swimming) and engineering applications (e.g., flow over airfoils or the motion of flexible structures). In IBM, the fluid domain is typically represented on a fixed Cartesian grid, while the solid boundaries are immersed within this grid. The fundamental concept is to impose the effects of the immersed boundaries on the surrounding fluid flow without conforming the grid to the shape of the object. This is achieved by employing special forcing terms in the Navier-Stokes equations that represent the boundary conditions at the interface between the fluid and the solid. Consequently, the immersed boundaries exert forces on the fluid, which are incorporated into the governing equations, enabling effective interaction between the fluid and the boundaries. A notable advantage of the Immersed Boundary Method is its capability to manage complex geometries and moving interfaces without the computational overhead associated with mesh generation and refinement, common in traditional methods like the FEM or FVM. In addition, IBM can easily accommodate substantial boundary deformations, making it suitable for simulating flexible structures and dynamic interactions. However, the accuracy of the method can be influenced by the choice of forcing functions and the grid resolution, particularly near the boundaries. Therefore, careful consideration of grid size and numerical scheme is essential to ensure accurate capture of interactions between the fluid and immersed boundaries.

Meshless Methods: Meshless methods represent a class of numerical techniques utilized to solve Partial Differential Equations (PDEs) without relying on a predefined grid or mesh as shown in Figure 2.5 . This allows for greater flexibility in handling complex geometries and dynamic problems. Instead of discretizing the domain, meshless methods utilize a set of scattered points within the computational domain to represent the solution. They approximate the governing equations by constructing local or global shape functions based on the values at neighboring points, enabling the computation of derivatives and integrals directly from the scattered data. This approach is particularly beneficial for problems involving large deformations, moving boundaries, or evolving interfaces, as it mitigates issues related to mesh generation and refinement. Meshless methods are increasingly employed in various fields, including fluid dynamics, structural analysis, and material science, offering a powerful alternative to traditional mesh-based techniques for simulating complex physical phenomena. A detailed summary is provided in Table 2.1.

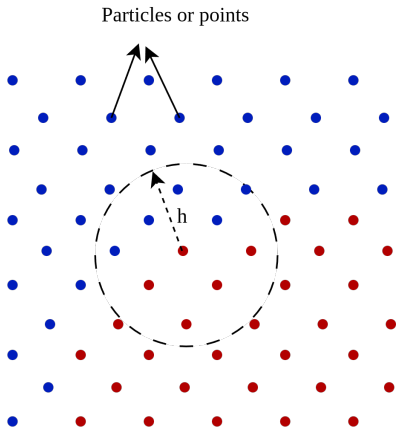

Figure 2.5: Representation of domain with particles or points for the meshless method

Smoothed Particle Hydrodynamics (SPH): SPH is a meshless, Lagrangian numerical method employed to simulate fluid flows and various continuum mechanics phenomena. Initially developed for astrophysical applications, SPH has gained prominence in diverse fields such as fluid dynamics, geophysics, and biomechanics due to its capability to effectively handle complex fluid interfaces and free surfaces. In SPH, the fluid is represented by a discrete set of particles, each possessing properties such as mass, position, velocity, and other relevant physical characteristics. The interactions between particles are governed by a kernel function that calculates the influence of neighboring particles. This smoothing approach enables the approximation of continuous fields, including density and pressure, without the necessity of a fixed grid. A primary advantage of SPH lies in its flexibility to manage large deformations, free-surface flows, and complex boundary conditions, rendering it well-suited for simulating phenomena such as fluid fragmentation, mixing, and solid-fluid interactions. Moreover, the absence of a mesh alleviates complications associated with mesh generation and refinement, particularly in dynamic simulations where the fluid domain may undergo significant alterations over time. Nonetheless, SPH is not without challenges, particularly concerning numerical stability. Maintaining accuracy during high-velocity impacts or in scenarios with strong gradients can be problematic. To address these issues and enhance the method's performance, various enhancements have been proposed, including kernel corrections and multi-resolution techniques.

Moving Particle Semi-Implicit (MPS): The MPS method is a numerical approach employed for simulating fluid flows and dynamic phenomena, with particular emphasis on free-surface flows and fluid-structure interactions. As a meshless Lagrangian technique, MPS does not rely on a fixed grid or mesh, providing enhanced flexibility in managing complex geometries and large deformations. In the MPS framework, fluid is represented by a collection of moving particles, each characterized by properties such as mass, position, velocity, and density. The interactions among these particles are computed utilizing a semi-implicit scheme that improves numerical stability. This method integrates explicit and implicit time-stepping techniques to solve the governing equations of fluid motion, allowing for effective management of stability during time integration—particularly beneficial when employing large time steps in dynamic simulations. A notable advantage of MPS is its efficacy in modeling free-surface flows, making it suitable for applications such as dam break simulations, sloshing in tanks, and other scenarios involving fluid motion and interfaces. Furthermore, the method can accommodate complex boundary conditions and moving objects with relative ease, a significant advantage over traditional mesh-based methods. Despite its merits, MPS faces limitations concerning particle distribution and potential numerical instability under certain conditions. Ongoing research seeks to enhance the robustness of the method through optimized particle arrangements and correction schemes aimed at improving accuracy.

Generalized Finite Difference Method (GFDM): GFDM utilizing meshless interpolation combine the advantages of finite difference techniques with the flexibility of meshless approaches for solving partial differential equations. In this framework, traditional finite difference schemes are generalized to accommodate irregular point distributions, allowing for more accurate derivative approximations without a fixed grid. Meshless interpolation techniques, such as Moving Least Squares (MLS) or radial basis functions, are employed to estimate field variables at non-grid points, enhancing the method's adaptability to complex geometries and boundary conditions. This approach proves particularly beneficial for simulating problems characterized by evolving interfaces or irregular domains, providing a robust and flexible tool applicable across a diverse range of fields, including fluid dynamics, heat transfer, and material science.

Finite Pointset Method (FPM): The FPM is a meshless numerical technique utilized for solving partial differential equations by representing the domain with a discrete set of points. In contrast to traditional mesh-based methods, FPM does not rely on a predefined mesh, allowing for enhanced flexibility in addressing complex geometries and dynamic interfaces. Within the FPM framework, the governing equations are solved by approximating field variables at pointset locations using local polynomial or radial basis function interpolations. The method incorporates a background grid to facilitate derivative integration and enforce boundary conditions. FPM is particularly well-suited for scenarios involving large deformations, fluid-structure interactions, and free-surface flows, establishing it as a valuable tool in engineering and scientific research for simulating intricate physical phenomena without the complications associated with mesh generation and refinement.

Feature	SPH	MPS	GFDM	FPM
Basic Concept	Interpolates physical quantities using smoothing kernels	Solves NS equations with semi-implicit formulations	Approximates derivatives using weighted least squares	Uses Taylor expansions for point cloud data
Domain Representation	Lagrangian particles	Lagrangian particles	Arbitrary point clouds (no connectivity)	Arbitrary point clouds (no connectivity)
Conservation Properties	Good mass conservation, challenges in momentum and energy	Good mass conservation, handles pressure better than SPH	Conservation depends on weighting functions	Conservation depends on Taylor series accuracy
Handling of Boundaries	Requires special techniques (ghost particles, kernel corrections)	Requires special boundary particles	Requires explicit boundary conditions	Handles boundaries with high flexibility
Numerical Diffusion	Moderate (depends on kernel and radius)	Low (better pressure calculations)	Depends on weighting schemes	Low (accurate derivative computation)
Accuracy	Moderate, sensitive to kernel choice and particle distribution	Moderate to high	High, flexible accuracy with higher-order derivatives	High, flexible accuracy for well-distributed points
Computational Cost	Moderate to high	Moderate to high	High (matrix assembly for weights)	High (matrix operations for Taylor expansions)
Grid Flexibility	Fully meshless, ideal for free-surface flows	Fully meshless, ideal for incompressible flows	Fully meshless, suitable for arbitrary geometries	Fully meshless, suitable for arbitrary geometries
Applications	Free-surface flows, astrophysics simulations	Incompressible flows, multiphase flows	General CFD, heat transfer, elasticity	General CFD, aeroacoustics, multiphysics
Advantages	Handles large deformations and free surfaces	Stable pressure and incompressible flows	High flexibility and accuracy for arbitrary geometries	High flexibility and accuracy for arbitrary geometries
Disadvantages	Sensitive to particle distribution, kernel choice	High computational cost for large systems	High computational cost, complex weighting schemes	High computational cost, complex setup for Taylor expansions

Table 2.1: Summary of meshless methods

2.3.4 Interface Tracking Methods for Grid Based Method

In grid-based methods for multiphase flow simulation, accurately tracking the interface between different phases is essential for capturing interfacial dynamics and phase interactions. The interface represents the boundary where properties like density, viscosity, and surface tension can vary sharply, and its accurate tracking is crucial to avoid artificial mixing and ensure realistic simulations. Several approaches are employed as shown in Figure 2.6 to handle this challenge, each with unique strengths and limitations. A detailed summary is provided in Table 2.2.

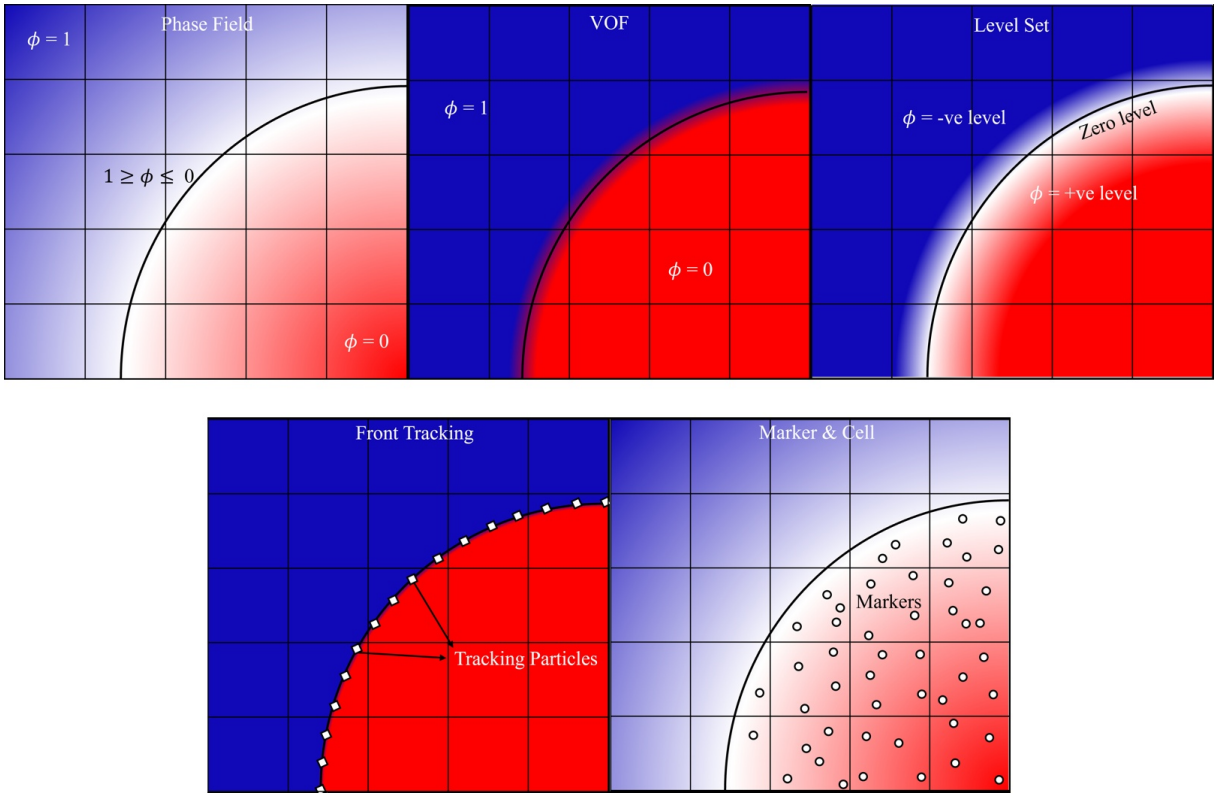

Figure 2.6: Interface tracking methods for gird based methods. Phase field: Diffuse (controlled by interface width), VOF: Diffuse (over a few cells), Level set: Sharp, but smeared numerically, Marker and cell: Diffuse using markers and Front tracking: Sharp interface using Lagrangian particle

Phase-Field Method: The Phase-Field method is an simple approach for capturing the interface, which models it as a diffuse region rather than a sharp boundary. This is achieved by introducing an order parameter (or phase field) that varies continuously across the interface, transitioning smoothly between values representing each phase. The evolution of this phase field is governed by the Cahn-Hilliard equation, which helps to model the motion and dynamics of the interface. The diffuse nature of the phase-field method makes it especially useful for simulations where the interface undergoes complex topological changes, such as merging or splitting, without requiring any special handling. However, one of the main limitations of the phase-field method is controlling the interface thickness, which can require fine grids to achieve high accuracy, increasing computational costs.

Volume of Fluid (VOF) Method: The Volume of Fluid (VOF) method is widely used in grid-based CFD simulations for tracking interfaces in multiphase flows. It represents the interface by defining a volume fraction field in each computational cell, which indicates the fraction of the cell occupied by a given phase. This volume fraction is a scalar value between 0 and 1, with intermediate values indicating the presence of the interface within the cell. To represent the interface shape more accurately, reconstruction techniques like Piecewise Linear Interface Calculation (PLIC) can be used to approximate the geometry of the interface. The VOF method is particularly effective for cases with large interfacial deformations, such as splashing or droplet breakup, and ensures mass conservation across the interface. However, a major challenge with VOF is that the interface can become smeared over multiple cells, especially in high-resolution cases, which can reduce the sharpness and accuracy of the captured interface.

Level Set Method: The Level Set method is a versatile technique for capturing interfaces in multiphase flows. It uses a signed distance function, where the value of the function represents the shortest distance to the interface, with positive values on one side and negative values on the other. The interface itself is the zero level set of this function. This implicit representation makes it easy to handle complex interfacial dynamics, including topological changes like merging and breaking. The Level Set function evolves over time to reflect the motion of the interface, using the level set equation. While this method provides a sharp, smooth interface, it can suffer from numerical inaccuracies due to the need for reinitializing the level set function periodically, which can introduce slight errors in the interface position.

Front-Tracking Method: The front-tracking method explicitly tracks the interface by using a separate set of markers or an independent mesh, typically represented as a collection of points or segments that define the interface boundary. These markers move along with the fluid velocity and are coupled with the Eulerian grid used for the fluid flow. This method maintains a highly accurate, sharp interface, making it especially useful for simulations involving surface tension and fine-scale interfacial details. However, the front-tracking method is computationally intensive, as it requires managing the interface markers separately and addressing complex topological changes, such as merging or breakup events. Despite these challenges, the front-tracking method is often chosen when a precise interface representation is needed for detailed interfacial phenomena.

Marker-and-Cell (MAC) Method: The Marker-and-Cell (MAC) method is an interface tracking technique that employs marker particles to distinguish different fluid regions and locate the interface. These particles are advected with the flow, marking the regions occupied by each phase, which helps in maintaining a sharp interface. The particle information is coupled with a grid-based solver that calculates fluid properties across the domain. The MAC method is particularly suitable for simulating free-surface flows, as it naturally captures the dynamic interface between the phases. However, it can be computationally demanding since it requires a high density of marker particles near the interface to maintain accuracy, which increases the computational load for high-resolution simulations.

Feature	Front Tracking	Marker-and-Cell (MAC)	Phase-Field Method	Volume of Fluid (VOF)	Level Set Method
Interface Representation	Explicit (Lagrangian markers)	Implicit (tracer particles)	Implicit (Cahn-Hilliard equation)	Implicit (volume fraction)	Implicit (distance function)
Interface Sharpness	Sharp, well-maintained	Diffuse	Diffuse (controlled by interface width)	Diffuse (over a few cells)	Sharp, but smeared numerically
Grid Setup	Eulerian + Lagrangian mesh	Eulerian (staggered grid)	Eulerian (uniform grid)	Eulerian (uniform grid)	Eulerian (uniform grid)
Handling of Surface Tension	Accurate	Less accurate	Accurate (surface tension in free energy)	Less accurate (special techniques required)	Accurate (gradient-based)
Numerical Diffusion	Minimal at interface	Higher at interface	Controlled by interface width	Moderate (depends on advection scheme)	Moderate (depends on reinitialization)
Complex Interface Topology	Challenging (merging/splitting)	Challenging	Easy (naturally handled by diffuse interface)	Easy (automatic via volume fractions)	Easy (automatic via level set evolution)
Mass Conservation	Good	Good	Poor (not strictly conserved)	Excellent (strictly conserved)	Poor (not strictly conserved)
Computational Cost	Moderate	Low	High (additional equations)	Moderate	High (additional equations)
Physical Basis	Explicit tracking via markers	Particle-based advection	Thermodynamic free energy	Volume fraction advection	Distance function advection
Applications	Sharp interface flows, high surface tension effects	General incompressible flows	Multiphase flows with diffuse interfaces	Multiphase flows with strict mass conservation	Multiphase flows requiring sharp interfaces

Table 2.2: Detailed summary of interface tracking methods for gird based methods. Phase field: Diffuse (controlled by interface width), VOF: Diffuse (over a few cells), Level set: Sharp, but smeared numerically, Marker and cell: Diffuse using markers and Front tracking: Sharp interface using Lagrangian particle

2.4 Surface Tension

Surface tension is a phenomenon that occurs at the interface between two phases, such as water and air as shown in Figure 2.7. It is the result of cohesive forces between liquid molecules, which cause the liquid surface to behave as if it were covered with a stretched elastic membrane. In the case of water, this tension is especially strong due to hydrogen bonding among water molecules. Water molecules in the bulk of the liquid are surrounded by other water molecules and experience attractive forces from all directions. However, molecules at the surface lack neighboring molecules in the air above. Consequently, these surface molecules experience a net inward pull due to cohesive forces from molecules within the liquid. This imbalance of forces causes the surface to contract, minimizing the surface area and creating a state of tension at the boundary. This tension manifests as surface tension, measured in units of force per unit length (e.g., N/m).

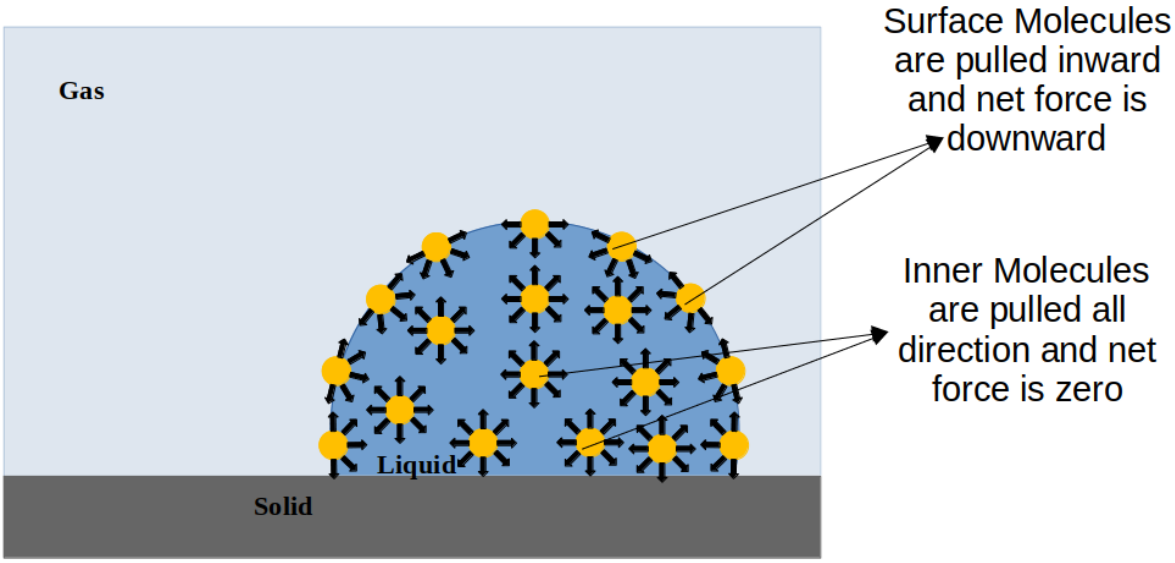

Figure 2.7: Representation of surface tension on liquid - air system.

Surface tension plays a critical role in multiphase flows, affecting phenomena such as droplet formation, interface stability, and capillary waves. Surface tension originates at the molecular level. However, the surface tension ($\mathbf{F}_s$) is a macroscopic parameter. An interface seeks to minimize its surface energy:

$$\text{Surface energy} = \mathbf{F}_s \times \text{Area} \tag{2.8}$$

Then surface tension is surface energy per unit area. It is also termed as force exerted at the interface per unit length. Several methods have been developed in CFD to model surface tension forces accurately. The most common methods are presented in below sections.

2.4.1 Continuum Surface Force (CSF)

The CSF method, developed by Brackbill et al. [19]. The CSF model represents surface tension effects in fluid dynamics by modeling the surface tension as a body force acting on the fluid. The force per unit volume due to surface tension is given by:

$$\mathbf{F}_s = \sigma\kappa\mathbf{n} \tag{2.9}$$

Where,

- σ is the surface tension coefficient
- $\mathbf{n}$ is the unit normal vector to the interface and
- κ is the local curvature

The curvature κ can be calculated using the gradients of the phase indicator function ϕ, which defines the interface between phases:

$$\kappa = \nabla \cdot \mathbf{n} \tag{2.10}$$

In practice, the CSF approach requires a method for determining the normal vector and curvature, often derived from the level-set function or a phase-field representation.

2.4.2 Smoothed Continuum Surface Force (Smoothed CSF)

The Smoothed CSF method is a modification of the standard CSF approach, aimed at improving numerical stability and interface capturing by smoothing the representation of the interface. In the Smoothed CSF, the surface tension force is computed over a region surrounding the interface rather than at the interface itself. The force is smoothed by employing a weighting function or kernel function $W(\mathbf{r})$:

$$\mathbf{F}_s = \int_\Omega \sigma\kappa\mathbf{n}W(\mathbf{r} - \mathbf{r}')\, d\mathbf{r}' \tag{2.11}$$

Where,

- Ω is the domain around the interface and
- $W(\mathbf{r} - \mathbf{r}')$ is a smoothing kernel.
- $\mathbf{r}$ is distance vector of the neighbour point
- $\mathbf{r}'$ is distance vector of the center point

This method allows for a more gradual transition in properties across the interface, reducing numerical oscillations and improving overall simulation stability.

2.4.3 Sharp Surface Force (SSF)

The Sharp Surface Force (SSF) approach focuses on accurately capturing the effects of surface tension without smoothing the interface. It is often used in simulations where maintaining a sharp interface is critical. In SSF, the surface tension force is applied directly at the interface, defined by a sharp indicator function ϕ that takes a value of 1 in one phase and 0 in the other. The force per unit volume is expressed as:

$$\mathbf{F}_s = \sigma\kappa\delta(\phi)\nabla\phi \tag{2.12}$$

Where, $\delta(\phi)$ is the Dirac delta function, ensuring that the surface tension is only applied at the interface. The force can also be represented using a Heaviside function $H(\phi)$ that distinguishes between the phases:

$$\mathbf{F}_s = \sigma\kappa\nabla H \tag{2.13}$$

2.5 Dynamic Contact Angle (DCA)

The contact angle is formed at the three-phase boundary where a liquid intersects with both a solid and a gas. It serves as a key measure of how well, or how poorly, a liquid will spread over a surface. For instance, in the formulation of coatings, inks, and paints, the contact angle provides a useful indication of how modifications to these materials might affect their spreading behavior. This measurement is critical not only for assessing the performance of the product but also for determining the success of the application process. The contact angle, typically denoted as θ, expresses the interaction between a liquid and a solid surface. For example, a liquid droplet on a solid surface creates an interface, and the contact angle formed at this interface provides insight into the degree of interaction between the two phases, as shown in Figure 2.8. The liquid's interaction with the solid

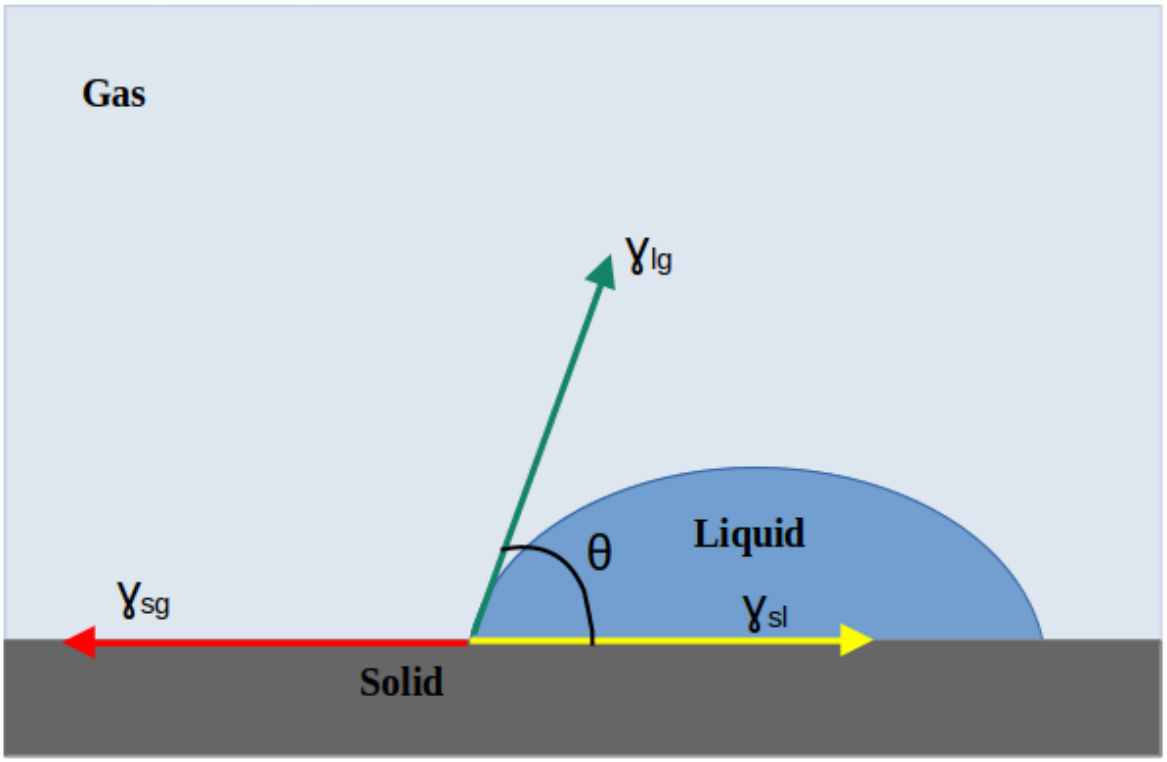

Figure 2.8: Represention of contact angle at the three phase boundary point

surface can be classified broadly into two categories:

1. **Non-wetting:** The contact angle is close to 180°, meaning the liquid tends to stay in droplet form and does not spread across the surface.

2. **Wetting:** The contact angle is close to 0°, meaning the liquid spreads completely over the surface, a phenomenon referred to as "perfect" or "complete" wetting.

Wettability is inversely proportional to the contact angle: the lower the contact angle, the higher the wettability. For most real-world cases, the contact angle lies between 0° and 180°. When $\theta = 90°$, the situation is neither fully wetting nor non-wetting. A contact angle less than 90° indicates wetting behavior, while an angle greater than 90° suggests non-wetting behavior. Based on contact angle measurements, surfaces can be classified into the following categories and shown in Figure 2.9:

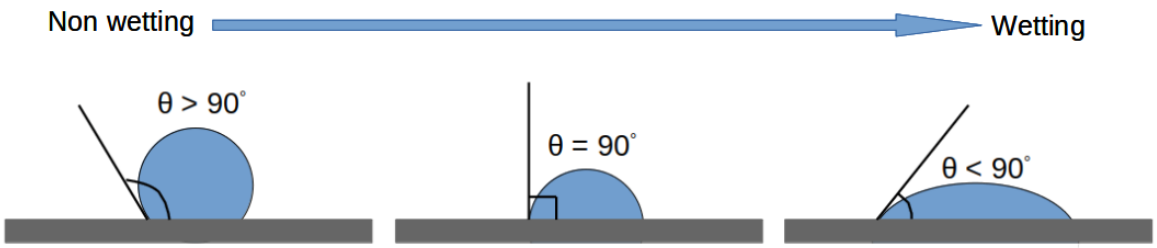

Figure 2.9: Classification of Surface and Wettability nature with respect to contact angle

1. **Hydrophilic:** Contact angle $< 90°$
2. **Hydrophobic:** Contact angle $> 90°$
3. **Superhydrophobic:** Contact angle $> 150°$

The size of the contact angle depends on the physical properties of the materials involved, including surface tension. A droplet's spherical shape is influenced not only by the nature of the surface but also by the surface tension of the liquid. Surface tension causes liquids, such as water, to form spherical droplets. This phenomenon occurs because particles within the liquid are attracted to each other, creating a force known as cohesion. When particles are surrounded by others of the same kind, the net force on each is zero. However, at the liquid's surface, there are no particles above to balance the forces, resulting in a net inward and downward pull. This creates a high-energy state at the surface, which drives the liquid into a spherical shape to minimize surface area—this is the essence of surface tension. Liquids with high surface tension tend to form larger contact angles and remain in droplet form, while those with low surface tension will exhibit smaller contact angles and spread more easily over solid surfaces. This can be summarized as follows:

1. **Non-wettability:** High surface tension leads to a large contact angle.
2. **Wettability:** Low surface tension results in a small contact angle.

Contact angle theory is rooted in surface tension, as described by the Young-Laplace equation. This equation calculates the contact angle by balancing the surface energies at the liquid-solid-gas interface

$$\gamma_{sg} = \gamma_{sl} + \gamma_{lg} \cos\theta$$

Where,

- θ is the contact angle,
- γ_{sg} is the solid-gas surface energy,
- γ_{sl} is the solid-liquid surface tension and
- γ_{lg} is the liquid-gas surface tension.

The properties of the solid surface play a crucial role in determining wettability. When the droplet is in equilibrium, the forces acting on it are balanced. The contact angle can then be expressed as:

$$\cos\theta = \frac{\gamma_{sg} - \gamma_{sl}}{\gamma_{lg}}$$

This equation shows how surface energies influence the contact angle:

1. If $\gamma_{sg} < \gamma_{sl}$, then $\cos\theta$ will be negative, resulting in $\theta < 90°$, indicating a wetting condition.

2. If $\gamma_{sg} > \gamma_{sl}$, then $\cos\theta$ will be positive, resulting in $\theta > 90°$, indicating a non-wetting condition.

Various methods have been developed in computational fluid dynamics (CFD) to model the dynamic contact angle. The most common approaches are presented in the sections below.

2.5.1 Kistler's Model

Kistler's model [20] describes the advancing contact angle (θ_A) as a function of the capillary number (Ca) and the equilibrium contact angle (θ_E), based on Hoffman's empirical function [21]:

$$\theta_A = f_H\left(Ca + f_H^{-1}(\theta_E)\right) \tag{2.14}$$

Where,

- θ_A is the advancing contact angle
- Ca is the capillary number
- θ_E is the equilibrium contact angle and
- $f_H(x)$ is Hoffman's function

Hoffman's function, $f_H(x)$, is defined as:

$$f_H(x) = \arccos\left(1 - 2\tanh\left(5.16\left(\frac{x}{1+1.31x^{0.99}}\right)^{0.706}\right)\right) \tag{2.15}$$

This model is commonly used to predict advancing contact angles but requires additional treatment for receding angles, which can be handled by coupling with another model.

2.5.2 Dynamic Receding Contact Angle Model

Nichita et al. [22] extended Tanner's empirical work to formulate a model for receding angles. This model relates the dynamic receding contact angle (θ_D) with the capillary number:

$$\theta_D = \left(\theta_R^3 - 72Ca\right)^{1/3} \tag{2.16}$$

Where, θ_R is the static receding contact angle. This approach is useful for simulations where receding angle dynamics are significant.

2.5.3 Shikhmurzaev's Model

Shikhmurzaev [23] proposed a model that links the DCA with the contact line velocity ($\mathbf{u}_{cl}$) and phenomenological constants:

$$\cos(\theta_D) = \cos(\theta_A) - \frac{2u(a_1 + a_2\mathbf{u}_0)}{(1 - a_2)\left((a_1 + \mathbf{u}_{cl}^2)^{1/2} + \mathbf{u}_{cl}\right)} \tag{2.17}$$

Where, $\mathbf{u_0}$ is radial velocity, a_1, a_2, and other parameters are fitted values specific to the fluid interface being studied. This model provides flexibility for applications involving varied wettability conditions.

2.5.4 Cox's Model

Cox's model [24] calculates both advancing and receding contact angles by incorporating the apparent contact angle (θ_{app}), the capillary number, apparent length (L) and the slip length (λ):

$$\theta_D = g^{-1}\left(g(\theta_{\text{app}}) + Ca\log\left(\frac{L}{\lambda}\right)\right) \tag{2.18}$$

Where, $g(\theta)$ is an integral function given by:

$$g(\theta) = \int_0^{\theta} \frac{x - \sin(x)\cos(x)}{2\sin(x)}\, dx \tag{2.19}$$

This model is especially useful when simulations require accurate handling of slip effects at the contact line.

2.5.5 Quasi-Dynamic Contact Angle Model

The quasi-dynamic model, as discussed by Göhl et al. [25], simplifies the contact angle behavior by setting a constant advancing angle (θ_A) and receding angle (θ_R) depending on the contact line motion direction:

$$\theta_D = \begin{cases} \theta_A & \text{if advancing} \\ \theta_R & \text{if receding} \end{cases} \tag{2.20}$$

This model is computationally efficient and applicable where experimental data for contact angle hysteresis is available, though it may lack the accuracy of more detailed models.

2.5.6 Yokoi's Model

The dynamic contact angle is modeled as a function of the contact line velocity $\mathbf{u}_{cl}$ and Tanner's law [22], combining capillary-dominated and inertia-dominated regimes[26]:

$$\theta(\mathbf{u}_{cl}) = \begin{cases} \min\left(\theta_E + \left(\frac{\text{Ca}}{k_a}\right)^{1/3}, \theta_{mda}\right), & \text{if } \mathbf{u}_{cl} \geq 0 \quad \text{(Advancing phase)}, \\ \max\left(\theta_E + \left(\frac{\text{Ca}}{k_r}\right)^{1/3}, \theta_{mdr}\right), & \text{if } \mathbf{u}_{cl} < 0 \quad \text{(Receding phase)}, \end{cases} \tag{2.21}$$

Where:

- $\theta(\mathbf{u}_{cl})$: Dynamic contact angle as a function of the contact line velocity $\mathbf{u}_{cl}$.
- Ca: Capillary number, defined as:

$$\text{Ca} = \frac{\mu \mathbf{u}_{cl}}{\sigma},$$

  Where, μ is the liquid dynamic viscosity, $\mathbf{u}_{cl}$ is the contact line velocity, and σ is the surface tension.
- θ_E: Equilibrium contact angle at zero velocity (Ca = 0).
- θ_{mda}: Maximum dynamic advancing angle.
- θ_{mdr}: Minimum dynamic receding angle.
- k_a, k_r: Material-dependent constants for the advancing and receding phases, respectively.

For the advancing phase ($\mathbf{u}_{cl} \geq 0$), the dynamic contact angle increases with $\mathbf{u}_{cl}$ and is capped at θ_{mda}. For the receding phase ($\mathbf{u}_{cl} < 0$), the dynamic contact angle decreases with $\mathbf{u}_{cl}$ but is limited by θ_{mdr}. This model captures the asymmetric nature of advancing and receding contact angles by using distinct constants (k_a, k_r) and dynamic limits ($\theta_{mda}, \theta_{mdr}$).

2.5.7 Davis–Hocking Model for Contact-Line Dynamics

The Davis–Hocking model describes the relationship between the dynamic contact angle θ and the contact-line velocity $\mathbf{u}_{cl}$ via the mobility parameter M. The fundamental equation is:

$$M\Delta\alpha = \mathbf{u}_{cl}, \tag{2.22}$$

Where, $\Delta\alpha = \theta - \theta_E$ is the difference between the dynamic contact angle and the equilibrium contact angle θ_E. In systems with contact angle hysteresis, the model expands as [27]:

$$\theta = \begin{cases} \theta_a + \frac{\mathbf{u}_{cl}}{M}, & \text{if } \mathbf{u}_{cl} > 0 \quad \text{(advancing)} \\ \theta_r + \frac{\mathbf{u}_{cl}}{M}, & \text{if } \mathbf{u}_{cl} < 0 \quad \text{(receding)}, \end{cases} \tag{2.23}$$

Where, θ_A and θ_R are the advancing and receding static contact angles, respectively. To ensure the dynamic contact angle remains physical, the following boundary condition is applied:

$$\theta = \max(\min(\theta, 180^\circ), 0^\circ). \tag{2.24}$$

This model captures the linear dependence of the dynamic contact angle on the contact-line velocity, incorporating material properties via the mobility parameter M.

2.6 Fluid-Structure Interaction (FSI)

Fluid-Structure Interaction (FSI) encompasses various methodologies for simulating the interaction between multiphase fluids and solid structures, which is critical in numerous engineering and scientific applications. These interactions become particularly complex in multiphase scenarios, where different fluid phases (such as liquid, gas, and particles) exert varying forces and moments on the structure. This complexity can significantly influence the dynamics of the system, affecting factors such as stability, performance, and material integrity. FSI problems involving multiphase flows are prevalent in fields such as automotive and industrial engineering (e.g., Noise-Vibration-Harshness (NVH)), chemical engineering (e.g., mixing of different fluids in reactors), environmental engineering (e.g., sediment transport in rivers), and biomedical engineering (e.g., the behavior of blood flow in the presence of air bubbles or emboli). The accurate modeling of these interactions is essential for predicting the behavior of the system under diverse operating conditions. Various methodologies, including fully coupled (monolithic) methods, partitioned methods, weak coupling, and strong coupling, are employed to tackle these challenges, each with its own set of advantages and limitations. As computational resources expand and numerical techniques evolve, the capability to simulate multiphase FSI with greater precision continues to advance, empowering engineers and researchers to develop more effective and resilient systems.

2.6.1 Fully Coupled (Monolithic) Methods

Fully coupled methods solve fluid and structural equations simultaneously within a unified framework, treating the interaction as a single problem. This approach provides high accuracy and robustness by accounting for the complex nonlinear behaviors of both fluid and structure. However, it is computationally intensive and requires sophisticated algorithms, making implementation more challenging.

2.6.2 Partitioned Methods

Partitioned methods divide the FSI problem into independent fluid and structure subproblems, solving each sequentially or iteratively. This flexibility allows for the use of specialized solvers for each component, which can be optimized separately. While this method reduces the initial computational cost and allows for scalability, it may encounter convergence issues and requires careful treatment of the interface to ensure accuracy. Weak and strong coupling can occur within both fully coupled (monolithic) methods and partitioned methods, but they have different implications depending on the context. In partitioned methods, weak coupling implies minimal interaction, while strong coupling means frequent data exchanges. In fully coupled methods, strong coupling is inherent due to simultaneous solving of the fluid and structural equations. Understanding these methodologies allows for better selection in engineering applications involving fluid-structure interactions.

2.6.3 Weak Coupling

Weak coupling features a loose interaction between fluid and structure, where data exchange occurs infrequently, typically at larger time intervals. This approach reduces computational effort and simplifies implementation, making it easier to utilize existing

solvers. However, it can lead to inaccuracies in scenarios with strong interactions, as it does not fully account for the fluid's effect on the structure or vice versa.

2.6.4 Strong Coupling

Strong coupling involves a tight interaction with frequent data exchange between fluid and structure solvers, allowing for a more accurate representation of their dynamics. This method enhances accuracy and convergence in highly dynamic systems, but it also significantly increases computational demands and complexity in implementation due to the need for close coordination between solvers.

2.6.5 Mode Superposition (Partitioned based weak coupling)

The method of modal superposition is employed to analyze the dynamic behavior of structures. It is estimated through the superposition of a limited number of modal frequencies obtained from the modal analysis. Modal analysis comes into play to determine the vibration characteristics, primarily the modes of operation and the natural frequencies of a mechanical system or component. Natural frequency, or eigenfrequency, denotes the frequency at which a system naturally oscillates without any external driving force. On the other hand, mode shapes, also referred to as eigenvectors, depict the inherent behavior of the component at its natural frequency. Both these parameters hold significance in the structural design process, especially for scenarios involving dynamic loads. This approach is particularly effective in minimizing computational efforts when evaluating the dynamic response of linear structures [28, 29]. This technique proves advantageous especially when dealing with limited known loading frequencies. However, it is less applicable to the issues that encompass exceedingly high frequencies [30, 31].

The dynamic equation for a structure can be represented in matrix form as follows:

$$\boldsymbol{M}\ddot{\boldsymbol{u}} + \boldsymbol{C}\dot{\boldsymbol{u}} + \boldsymbol{K}\boldsymbol{u} = \boldsymbol{f}\,(t) \tag{2.25}$$

In this equation, $\boldsymbol{M}$ denotes the mass-normalized matrix, $\boldsymbol{C}$ represents the damping matrix, and $\boldsymbol{K}$ stands for the stiffness matrix. The column vector $\boldsymbol{u}$ corresponds to the degree of freedom, while $\boldsymbol{f}(t)$ represents the applied forces over time. These matrices are obtained through the discretization of the physical domain, resulting in an NxN matrix where N signifies the degrees of freedom of the structural model. Mass normalization is convenient in the modal superposition, as it ensures that the modal mass is consistent across all modes, simplifying the modal participation factors and making them directly interpretable as a percentage of total mass.

The foundation of modal superposition is rooted in modal analysis, yielding essential outputs such as eigenfrequencies and their corresponding mode shapes. The eigenfrequencies are computed via the undamped dynamic equation, treated as an eigenvalue problem:

$$(-\omega^2\boldsymbol{M} + \boldsymbol{K})\boldsymbol{\Phi} = 0, \qquad \boldsymbol{\Phi} \neq 0 \tag{2.26}$$

In this context, the symbol $\boldsymbol{\Phi}$ refers to the modal matrix, which contains a vector of the mode shape corresponding to every natural frequency of the structure with n-DOF, $\boldsymbol{\Phi} = \boldsymbol{\Phi}_1, \boldsymbol{\Phi}_2, ..., \boldsymbol{\Phi}_n$. Usually, the Finite Element Method (FEM) is used to model a structure, and discretize and solve Equation (2.26). Multiple numerical methods exist for determining natural frequencies and mode shapes, as no single method is universally optimal for all problems. The techniques for extracting eigenvalues fall under the category

of transformation methods and/or tracking methods. The eigenvalue equation is initially converted into a specific format in the transformation method, facilitating the extraction of eigenvalues. The tracking method involves extracting the eigenvalues individually through an iterative procedure. In this study, the Lanczos method was used, which combines characteristics of the tracking and transformation methods. Mass normalization involves scaling the mode shapes such that the square of the mode shape integrated over the structure equals one. This ensures that each mode shape has a unit mass and simplifies the subsequent modal superposition calculations.

After the vibration modes and frequencies are extracted, their combination may be used to simulate complex vibration of the structure. The superposition involves expressing the displacement response as a linear combination of modal contributions. The overall displacement ($\boldsymbol{u}(t)$) of the structural system for a time step can be represented as a combination of mode shapes:

$$\boldsymbol{u}(t) = \sum_{i=1}^{n} \boldsymbol{\Phi} \boldsymbol{y_i}(t) \tag{2.27}$$

Where, $\boldsymbol{y}(t)$ is the vector of modal coordinates (or generalized displacement). While one can extract many vibration modes from a FEM model, in engineering practice, usually only first few modes are relevant for analysis. By applying the generalized displacement and the mass normalized modal vector $\boldsymbol{\Phi}$ (i.e., substituting Equation (2.27) into Equation (2.25)), the following is obtained:

$$\boldsymbol{\Phi}^T \boldsymbol{M} \boldsymbol{\Phi} \ddot{\boldsymbol{y}}(t) + \boldsymbol{\Phi}^T \boldsymbol{C} \boldsymbol{\Phi} \dot{\boldsymbol{y}}(t) + \boldsymbol{\Phi}^T \boldsymbol{K} \boldsymbol{\Phi} \boldsymbol{y}(t) = \boldsymbol{\Phi}^T \boldsymbol{f}(t) \tag{2.28}$$

To decouple the equation of motion for a Multi-Degree-of-Freedom (MDOF) system into n equations of motion for Single Degree of Freedom (SDOF) systems, it is necessary to diagonalize the damping term. This requires the introduction of a damping matrix, as proposed by Lord Rayleigh, that is assumed to exhibit proportionality to both the mass, stiffness matrices with Rayleigh constants (β, α).

$$\boldsymbol{C} = \beta \boldsymbol{K} + \alpha \boldsymbol{M} \tag{2.29}$$

The final equation of motion to be solved to simulate the FSI is given as follows:

$$\ddot{\boldsymbol{y}}_i(t) + 2\omega_i \zeta_i \dot{\boldsymbol{y}}_{\boldsymbol{i}}(t) + \omega_i^2 \boldsymbol{y}_i(t) = \boldsymbol{\Phi}_i^T \boldsymbol{f}(t) \tag{2.30}$$

Where, ζ_i represents the damping ratio associated with mode i. It signifies the extent of real damping present within a system in comparison to critical damping.

While any integration method may be used to solve the above ordinary differential Equation (2.30) (ODE), in this proposed coupling method, the equation is solved using the Complementary Function and Particular Integral (CFPI) method [31]. The solution is presented in two parts: the complementary solution and the particular solution.

The complementary solution is defined as:

$$\begin{aligned} \boldsymbol{y}_t &= \boldsymbol{y_{t-1}} \cdot e \cdot (C + \frac{\zeta}{s} \cdot S) + \dot{\boldsymbol{y}}_{\boldsymbol{t-1}} \cdot e \cdot \frac{1}{\omega_n \cdot s} \cdot S \\ \dot{\boldsymbol{y}}_t &= \dot{\boldsymbol{y}}_{\boldsymbol{t-1}} \cdot e \cdot (C - \frac{\zeta}{s} \cdot S) - \boldsymbol{y_{t-1}} \cdot e \cdot \frac{\omega_n}{s} \cdot S \end{aligned} \tag{2.31}$$

where, $\boldsymbol{y}_t$ is displacement of current time step, $\boldsymbol{y}_{t-1}$ is displacement of previous time step, $\dot{\boldsymbol{y}}_t$ is velocity of current time step and $\dot{\boldsymbol{y}}_{t-1}$ is velocity of previous time step

The particular solution is defined as:

$$\begin{aligned}\boldsymbol{y}_t = &-e \cdot \boldsymbol{F_{t-1}} \cdot \left(\frac{\zeta \cdot \omega_n \cdot dt + 2 \cdot \zeta^2 - 1}{{\omega_n}^2 \cdot \mathrm{W}} \cdot S + \frac{\omega_n \cdot dt + 2 \cdot \zeta}{{\omega_n}^3 \cdot dt} \cdot C \right) \\ &+ \boldsymbol{F_{t-1}} \cdot \frac{2 \cdot \zeta}{{\omega_n}^3 \cdot dt} + e \cdot \boldsymbol{F_t} \cdot \left(\frac{2 \cdot \zeta^2 - 1}{{\omega_n}^2 \cdot \mathrm{W}} \cdot S + \frac{2 \cdot \zeta}{{\omega_n}^3 \cdot dt} \cdot C \right) \\ &+ \boldsymbol{F_t} \cdot \frac{\omega_n \cdot dt - 2 \cdot \zeta}{{\omega_n}^3 \cdot dt} \\ \dot{\boldsymbol{y}}_t = &\; e \cdot \boldsymbol{F_{t-1}} \cdot \left(\frac{\zeta_i + \omega_n \cdot \mathrm{dt}}{\omega_n \cdot wts} \cdot S + \frac{1}{{\omega_n}^2 \cdot \mathrm{dt}} \cdot C \right) - \boldsymbol{F_{t-1}} \cdot \frac{1}{{\omega_n}^2 \cdot \mathrm{dt}} \\ &- e \cdot \boldsymbol{F} \cdot \left(\frac{\zeta_i}{\omega_n \cdot wts} \cdot S + \frac{1}{{\omega_n}^2 \cdot \mathrm{dt}} \cdot C \right) + \mathrm{F} \cdot \frac{1}{{\omega_n}^2 \cdot \mathrm{dt}}\end{aligned} \tag{2.32}$$

The following coefficients are introduced for easier readability of the equations:

$$\begin{aligned} s &= \sqrt{1 - \zeta^2} \\ W &= \omega_n \cdot dt \cdot s \\ e &= \exp(-\zeta \cdot \omega_n \cdot dt) \\ S &= \sin(W) \\ C &= \cos(W) \end{aligned} \tag{2.33}$$

The final solution is obtained as the sum of both complementary solutions and particular solutions. The CFPI method of integration was chosen in this study, because it was verified that it is less sensitive to numerical errors when solving high-frequency oscillations, as compared to the Newmark-beta method [31]. Since the vibration of the structure is simply obtained using the direct integration of deformation and velocity value for each mode, the time-step used for CFPI integration may be decoupled to fluid solver time-step criterions. In other words, the high frequencies of the structural vibrations may be accurately reproduced while interacting with fluid flow.

3 Literature Review

3.1 Relevant Studies - Lagrangian Differencing Dynamics (LDD)

Initially, Basic et al. [32] established the foundational theoretical framework with their study of meshless renormalized Laplacians for boundary value problems, setting the stage for novel Lagrangian methods to simulate free surface flows, which is called Lagrangian Differencing Dynamics (LDD). It stands out from other major meshless methods, which typically prioritize conservation first and then focus on solution consistency. In contrast, the LDD method begins with a unique approximation scheme to ensure accurate gradient and Laplacian operators with second-order consistency. This approach allows for a smaller support domain, resulting in higher computational efficiency. Additionally, LDD incorporates a position-based point regularization scheme that is unconditionally stable and ensures conservation throughout the solution process. Furthermore, its novel boundary treatment requires only a surface mesh, simplifying boundary handling compared to traditional methods. The equations are solved in a fully mesh-free manner, with implementations that are fully parallelized on both GPU and CPU, maximizing computational speed and scalability. The solution of a time step in the LDD method initiates with the Lagrangian advection of points, i.e., the points are moved in space according to their velocities. The streamlines compressibility issues that arise during Lagrangian advection are resolved using the Particle-Based Dynamics (PBD) technique, which iteratively rearranges the locations of points by enforcing a uniform distances between neighbor points [33]. Following this, the pressure Poisson Equation (PPE) defined above is discretized by using the discrete operators, that are defined above and analyzed in [34]. In this study, the PPE is solved using the preconditioned BiCGSTAB linear solver, as explained in [33]. This groundwork was expanded and applied the LDD technique to sloshing simulations, demonstrating the method's capability in addressing complex fluid dynamics problems [35]. The approach was further extended to predict green water loadings, showcasing its effectiveness in maritime applications with wave impacts and fluid loadings. Subsequent advances, the refined method for incompressible flow dynamics, broadening its applicability to various fluid flow scenarios [36]. Integration with structural analysis was explored by Basic et al. [37], who coupled meshless non-Newtonian fluid flow integrated with structural solvers, illustrating the method's versatility. Further diversified the application of LDD to granular flow modelling, expanding its use beyond fluids to granular materials [38]. Recent developments by Paneer et al. [39, 40] have refined LDD for the elastic behaviour of structures and fluid-structure interactions, respectively. Johannes et al. [41] developed a GPU-powered finite difference solver, using a generalized approach for incompressible multiphase flows using a Riemann solver. The approach features a dampening scheme that handles high-density ratios using LDD Laplacian, as introduced in [32].

3.2 Relevant Studies - Multiphase

Multiphase flow dynamics is a complex and highly specialized area of study that focuses on the interactions between different fluids separated by a thin interface layer. This interface can exhibit intricate and dynamic behavior as the various fluid phases interact, often leading to complex flow patterns. The accurate modeling and simulation of these interfaces are essential in many engineering and scientific applications, including fluid-structure interactions, industrial processes, and environmental modeling. Specialized techniques and advanced mathematical frameworks are employed to capture and simulate these interfaces, especially in Eulerian frameworks.

In Eulerian approaches, the challenge lies in capturing the interface between fluids, given that these methods work on a fixed grid. One prominent technique used to represent the interface in this framework is the Phase Field method, first described by Cahn and Hilliard [1]. This method introduces a continuous field variable that implicitly represents the interface as a diffuse region, where the properties of the fluid vary gradually across the interface. This technique allows for a smooth transition between different phases and has been widely adopted due to its simplicity in modeling the dynamics of phase transitions. Another widely used technique is the Volume of Fluid (VOF) method, introduced by Hirt and Nichols [2]. The VOF method tracks the interface using a fractional volume function that indicates the proportion of each fluid present in each mesh element. It provides a good balance between computational efficiency and accuracy, especially for cases where the interface is relatively stable and does not exhibit sharp or highly dynamic changes. The Level Set method, introduced by Osher and Sethian [42], offers a different approach to interface tracking. This method employs a signed distance function to implicitly define the boundary of the interface as the zero-level set, providing a robust way to handle complex interface shapes. Sussman et al. [3] further improved the Level Set method by enhancing its ability to handle two-phase flows, particularly in cases with high-density ratios and surface tension, thus improving its accuracy and efficiency in complex fluid dynamics scenarios involving air and water. The Front Tracking method, developed by Unverdi and Tryggvason [43], is another approach that explicitly tracks the interface using marker points that define its position. This method is particularly useful in simulations where the interface experiences large displacements and deformation. An advanced variant of these methods is the Conservative Level Set method [44], which integrates the features of both the VOF and Level Set methods to enhance mass conservation and effectively handle complex interface dynamics. More recent developments, such as the method introduced by Theillard et al. [5], simulate incompressible two-phase flows using a sharp interface approach. This method incorporates adaptive Cartesian grids for improved resolution and includes capillary forces in the pressure correction to maintain stability, even in complex and dynamic fluid interactions. Kamran et al. [45] proposed a combination of the Extended Finite Element Method (XFEM) with the Particle Level Set (PLS) method, providing an effective solution for simulating multi-fluid flows in engineering applications.

In contrast to Eulerian methods, Lagrangian methods naturally track fluid interfaces by following the motion of fluid particles or parcels, which inherently captures the interface dynamics without the need for separate interface-tracking techniques. The most well-known Lagrangian method is Smoothed Particle Hydrodynamics (SPH), which was initially developed by Gingold and Monaghan [46] and Lucy [47]. In SPH, the fluid is represented by discrete particles that carry physical properties such as density, pressure, and velocity, and these particles interact with each other based on a smoothing kernel. This method is highly flexible and can handle large deformations and free surface

flows. However, numerical instabilities can arise in certain multiphase flows due to particle interaction, especially in cases involving sharp interfaces and high-density contrasts. The Moving Particle Semi-Implicit (MPS) method [48] is another particle-based method that improves stability through semi-implicit time-stepping schemes, offering better performance in simulating complex free surface and multiphase flows. The Element-Free Galerkin (EFG) method [49], unlike traditional mesh-based methods, does not rely on a fixed grid but uses nodes to represent the fluid and solve the governing equations. While Lagrangian methods have several advantages, such as better capturing the movement of the interface, they can suffer from numerical instabilities, particularly in multiphase flows where large variations in density or viscosity occur. The Particle Finite Element Method (PFEM), also Lagrangian-based, is another technique where particles represent material points, and an updated finite element mesh is generated dynamically at each time step [50]. This method provides a flexible way to solve fluid dynamics problems but can be computationally expensive.

Over time, significant advancements have been made to overcome the limitations of these methods in multiphase flow simulations. SPH, which has been foundational in fluid simulation since its early developments by Gingold and Monaghan [46] and Lucy [47], has undergone significant improvements, especially in its ability to handle high-density contrasts and complex free-surface flows. Enhancements in kernel functions [51, 52] have allowed for better precision and stability in simulations involving multiphase fluids. The initial SPH models that addressed multiphase flows with density variations [6] have evolved into more sophisticated techniques that handle particles of varying densities, enabling realistic interactions between different fluid phases. This has made SPH particularly useful in astrophysical applications, such as simulating galaxy formation and fluid interactions in mixed-density environments [53]. Hu and Adams [54] applied SPH to capture macroscopic and mesoscopic flows, effectively dealing with density contrasts and interfacial dynamics. Further developments, such as the Hamiltonian interface SPH formulation by Grenier et al. [55], improved the method's ability to handle flows involving different fluids and free surfaces. In addition, Monaghan et al. [56] developed a robust SPH algorithm for immiscible flows, stabilizing interfaces and adjusting pressure for high-density ratios. Rezavand et al. [57] introduced an ISPH (incompressible SPH) scheme that used repulsive forces to maintain sharp interfaces and improve stability in complex multiphase flows, while later improvements by Rezavand [58] addressed the challenges of violent multiphase flows, enhancing both stability and accuracy. Shimizu et al. [59] applied ISPH to model oil spills, incorporating additional models for oil-water mixing and turbulence. Olejinik et al. [60] focused on resolving wetting phenomena within SPH, and Vacondio et al. [61] identified several challenges within SPH numerical schemes, particularly in improving computational efficiency and robustness. Recent advancements also include the development of a multi-scale SPH framework for simulating multiphase interactions between fluids and structures [62], enabling more detailed and accurate simulations of real-world problems.

Similarly, the MPS method, which was first introduced by Koshizuka and Oka [48], has also seen significant advancements for multiphase flow simulations. Guangtao Duan extended the MPS method into a multiphase framework called Multiphase MPS (MMPS), which is specifically designed to handle fluids with varying viscosities and densities. Duan introduced two key stabilization techniques: MMPS-HD (harmonic density) and MMPS-CA (continuous acceleration), to address instabilities at the fluid interface by modifying particle interactions. These techniques have been validated through numerous simula-

tions, and the MMPS-CA method has shown superior performance, especially when handling high-density and viscosity ratios [7]. Despite these improvements, the MPS method still faces challenges in simulating violent multiphase flows. To further address these issues, enhancements such as using a Laplacian operator with error-free first-order derivatives in MMPS have been introduced, improving the stability and accuracy of the method in complex flow scenarios [63]. A detailed summary of the study on multiphase systems is presented, along with relevant literature, as shown in the Table 3.1.

Method	Description
Phase Field Method	Uses a continuous field variable to represent the interface as a diffuse region, allowing a smooth transition between phases [1].
Volume of Fluid (VOF)	Tracks the interface using a fractional volume function, representing the proportion of each fluid in mesh elements [2].
Level Set Method	Uses a signed distance function to implicitly characterize the interface at the zero-level set [42].
Improved Level Set	Enhances the original Level Set method for handling high-density ratios and surface tension effects [3].
Front Tracking	Directly tracks the interface using marker points to explicitly define interface positions [43].
Conservative Level Set	Combines VOF and Level Set methods for improved mass conservation and complex interface dynamics [44].
Sharp Interface Level Set	Integrates modified pressure correction and adaptive grids, incorporating capillary forces into pressure estimation for high stability [5].
XFEM with Particle Level Set	Uses extended finite element with particle level set to simulate multi-fluid flows, handling complex interfaces and boundary interactions [45].
Smoothed Particle Hydrodynamics (SPH)	Particle-based, using smoothing kernels for properties like density and pressure, suited for free-surface flows and astrophysics [46, 47, 51, 52, 6, 53, 54, 55, 56, 57, 58, 59, 60, 61, 62].
Moving Particle Semi-implicit (MPS)	Particle-based method with semi-implicit time stepping, ensuring stable calculations for incompressible flows with complex interfaces [48, 7, 63].
Particle Finite Element Method (PFEM)	Combines particle and finite element approaches, where particles represent material points, used for remeshing and solving governing equations [50].

Table 3.1: Summary of study on Multiphase methods and literature reviews

3.3 Relevant Studies - Surface Tension and Dynamic Contact Angle

Surface tension plays a vital role in multiphase flow simulations, and various methods have been developed to model it effectively, each with its own strengths and applications. The Continuum Surface Force (CSF) method treats surface tension as a body force distributed across the interface, enabling a robust handling of interface dynamics without explicitly tracking the interface position, which makes it well-suited for simulating complex fluid behaviors in large-scale simulations [19]. In contrast, sharp interface methods directly apply the Young-Laplace equation to impose pressure jumps across interfaces, making them particularly suitable for scenarios where precise interface tracking and resolution are required, such as in simulations of droplet dynamics or bubble formation [4]. The Ghost Fluid Method (GFM) utilizes ghost cells to impose jump conditions for variables near the interface, ensuring an accurate representation of discontinuities in physical properties like pressure and velocity, which is beneficial in capturing sharp interface behavior and reducing numerical errors near the boundary [64]. Diffuse Interface Models (DIM) represent the interface as a smooth transition between phases, effectively avoiding explicit interface tracking while still capturing interfacial phenomena such as capillary waves and phase separation, making them ideal for systems where the interface is less distinct or more diffusive in nature [65]. The Lattice-Boltzmann Method (LBM) introduces surface tension through modified particle interactions, enabling the simulation of complex geometries and fluid behavior in systems with intricate boundaries, such as porous media or microfluidic devices [66]. Lastly, Smoothed Particle Hydrodynamics (SPH) employs a meshless approach to calculate surface tension forces among particles, excelling in scenarios with significant interfacial deformation, such as free-surface flows, and offers flexibility in handling large-scale simulations with adaptive resolution and dynamic interfaces [67]. Each of these methods has its own set of advantages and trade-offs, making them suitable for different types of multiphase flow problems.

Dynamic contact angle (DCA) models are essential for accurately simulating multiphase flow systems, especially where wetting dynamics are complex and vary with surface interactions and fluid velocities. The first rigorous description of the contact angle was introduced by Young in 1805, who described the static contact angle as the equilibrium state of a droplet on a solid surface, now famously expressed by Young's Equation [68]. However, Young's equation applied only to static, equilibrium conditions, without addressing the concept of dynamic contact angles. Shortly after, Pierre-Simon Laplace extended the understanding of capillary action in 1806 by formulating the Young-Laplace equation, which relates the pressure difference across a curved liquid interface to the surface tension [69]. In the early 20th century, scientists began exploring how the contact angle behaves when the contact line moves. Harkins and Jordan (1930) were among the first to demonstrate that the contact angle changes when a liquid moves across a surface, introducing the concept of contact angle hysteresis, where the advancing contact angle is larger than the receding contact angle [70]. Blake and Haynes (1969) furthered this by studying liquid-liquid displacement kinetics, focusing on how interfacial properties and dynamic contact angles impact fluid movement in capillaries [71]. A major theoretical breakthrough occurred with Joanny and de Gennes (1984), who proposed a model for the dynamic contact line. They suggested that the contact angle depends not only on surface tension but also on the speed at which the contact line moves, with faster movement leading to a greater deviation from the static contact angle [72]. Charles Extrand and

Alan Shapiro (1995) further advanced the understanding of dynamic wetting by systematically studying contact angle hysteresis. They observed that when a liquid advances across a surface, it encounters greater resistance due to surface roughness or chemical heterogeneity, leading to a larger contact angle. Conversely, during receding, the contact angle is smaller [73]. Another important theoretical advancement came with the Cox-Voinov law (1976), which relates the dynamic contact angle to the velocity of the moving contact line through a logarithmic correction term, particularly useful for low-speed wetting scenarios such as in coating flows [74]. Cox extended the model to calculate both advancing and receding dynamic contact angles by accounting for the capillary number and apparent contact angle, including physical slip length, thereby improving the representation of viscous forces and surface interactions [24]. Tanner's empirical correlation (1979) laid one of the early foundations for describing receding contact angles based on the capillary number, influencing subsequent models dealing with contact line dynamics in multiphase flow [22]. Kistler's Model (1993), leveraging Hoffman's empirical function [21], relates the dynamic contact angle to the capillary number and static contact angle, widely applied for advancing angles. Adaptations of this model also allow for the prediction of receding angles [20]. Shikhmurzaev's Model (1997) links the dynamic contact angle to the contact line velocity and phenomenological constants, offering versatility for complex fluid behaviors on surfaces with varying wettabilities [75]. The Dynamic Receding Contact Angle Model (2010), introduced by Nichita et al., extended Kistler's model to provide a cubic-root function-based approach for receding contact angles, combining Kistler's model with Tanner's correlation to describe receding behavior in multiphase flow [76]. Yokoi et al. (2009) proposed a model for dynamic contact angles that describes the angle as a function of contact line velocity, incorporating capillary and inertia-dominated regimes. Their model uses Tanner's law for low velocities and applies maximum/minimum dynamic angles for high velocities, ensuring asymmetry between advancing and receding phases for more accurate droplet behavior predictions [26]. The Quasi-Dynamic Contact Angle Model (2015) simplifies the modeling process by employing fixed advancing and receding angles based on experimental data. While less computationally demanding, its accuracy relies heavily on the availability of detailed experimental data [77]. Snoeijer and Andreotti (2013) introduced the concept of contact line friction, a molecular-scale interaction that resists the motion of the contact line, providing a more refined understanding of dynamic wetting by linking microscopic molecular forces to macroscopic observations [78]. Ludwicki et al. (2022) investigated whether the contact-line mobility parameter, which describes the relationship between the dynamic contact angle and contact-line velocity, is a material parameter, using both experimental and numerical approaches to study binary sessile drop coalescence on various surfaces [27]. These models and developments have greatly enhanced our understanding of dynamic wetting behavior in multiphase flow and continue to be integral in improving the accuracy of simulations in various industrial and scientific applications.

3.4 Relevant Studies - Fluid–Structure Interaction (FSI)

Fluid–Structure Interaction (FSI) is a prevalent physical phenomenon with significant relevance across various engineering applications, particularly in systems where fluid and structural dynamics are coupled. Some of the most important applications include the interaction between waves and vegetation in coastal wetlands, and wave–ice interactions in the Arctic environment, both of which are crucial in mitigating coastal flooding and understanding the dynamics of extreme environments [79], [80]. FSI plays a pivotal role in optimizing structural designs to ensure performance under fluid loads, contributing to the efficiency and reliability of designs for offshore installations, windmills, and ships [81]. Identifying FSI-related issues early in the design phase can lead to cost-effective design changes, minimizing the need for costly modifications during manufacturing or operation [82]. Additionally, FSI is a critical factor in the hydrodynamic performance of propellers, as evidenced in recent studies [83], [84]. In these systems, damping represents the energy dissipation within vibration cycles and plays a key role in resonance phenomena, significantly affecting vibration amplitudes and the number of notable vibrations in time-dependent scenarios. While the role of damping is often negligible in slightly damped vibrations, it becomes pronounced near resonant frequencies, where excitation is largely balanced by damping. In such cases, structural damping is generally low except at resonance, when vibration cycles maintain substantial independence [85].

However, simulating FSI effectively is a complex task that requires specific assumptions in both structural and fluid simulations. In most Computational Fluid Dynamics (CFD) simulations, elastic deformation at the boundaries is typically ignored [33], while in structural simulations, a constant pressure is usually assumed for both the interior and exterior boundaries. Paik et al. [86] developed methods for coupling CFD solvers with rigid and elastic models of a ship hull to compute structural loads. They employed one-way and two-way coupling approaches to model the ship as elastic. In one-way coupling, CFD forces are used for structural load analysis, but deformations are not fed back into the CFD solution. In contrast, two-way coupling incorporates hull deformations into the CFD solution. A URANS/DES overset solver coupled with the modal superposition method was used for these analyses, with a gluing method applied to transfer forces and deformations between non-matching CFD and structural grids [86].

Several approaches have been proposed to tackle the intricacies of one-way and two-way coupling in FSI. A prominent method is the fully coupled (monolithic) approach, which integrates both structural and fluid calculations within a single solver [87, 88]. However, conventional CFD solvers generally use an Eulerian-based approach, while structural formulations often rely on a Lagrangian-based approach. This results in a computational stiffness mismatch between the fluid and structural components, making extensive scenarios computationally intensive [89]. As a result, grid-based partitioned methods have gained popularity as a more feasible alternative. These methods solve fluid and structural formulations on different meshes using distinct solvers [90], but require effective communication protocols at the interface to transfer fluid loads to the structural mesh and vice versa. Mesh-based solvers also require careful manipulation of adjacent mesh nodes to prevent mesh entanglement or deformation when adjusting fluid mesh boundaries [91], [92]. Recent developments have successfully applied partitioned methods, such as coupling thin-walled girder theory with potential flow theory [28, 93] and linking modal structure solvers with RANS-VOF solvers and Boundary-Integral Equation Methods [94]. Solid4Foam, integrated with OpenFOAM, is one such method used for solving FSI problems [95, 96].

The meshless-based partitioned method has proven to offer several advantages, especially in scenarios involving free surfaces, violent flow, complex models, and large deformations [97]. By avoiding the need for re-meshing the model after deformation, it becomes highly effective in simulating complex fluid-structure interactions. FSI is achieved by coupling Smooth Particle Hydrodynamics (SPH) with structural solvers such as the Finite Element Method (FEM) [98, 99, 100] and Discrete Element Method (DEM) [101, 102, 103] to compute structural deformation. However, transferring information between the fluid and structural solvers is not trivial, as it is necessary to resolve the interfacial energy balance [104]. Although solving structural deformation using this method is computationally expensive, it is generally more efficient than the monolithic approach.

In recent years, the Mode Superposition method has gained popularity due to its robustness, speed, and computational efficiency in solving structural deformation. Debrabandere et al. (2012) introduced a reduced-order modeling approach for FSI simulations, using modal analysis to represent structural dynamics. The method solves the modal equations within the CFD solver using a complementary function and a particular integral method, achieving good results for simple test cases and demonstrating potential for efficient aeroelastic analysis of flexible structures in turbomachinery configurations [31]. Sun et al. (2019) applied the Moving Particle Semi-implicit (MPS) method in combination with the mode superposition technique to simulate violent hydroelastic phenomena [105], while Corrado et al. (2020) validated a two-way coupling approach between CFD and FEM solvers using the HIRENASD test case [30]. Modal superposition is a widely used and valuable technique due to its simplicity and computational efficiency, although its accuracy diminishes when large structural deformations occur. This is because the method assumes linear behavior and uncoupled modes, which may not hold true in cases involving significant nonlinearity or mode coupling. Despite these limitations, modal superposition remains effective for evaluating structures subjected to dynamic loads within its valid range [31, 105, 30].

Weak coupling in FSI provides simplicity and ease of implementation, making it suitable for transient events. However, it has limitations, including stability issues requiring small time steps, which can lead to computational inefficiency, especially in large-scale simulations where fluid and structural solvers may require time steps of different magnitudes. Despite these challenges, the mode superposition approach allows the structural solver to add minimal computational cost, enabling better alignment with the flow solver's time step requirements [106], [31], [93].

4 Conclusion and Future Work

This paper provides an overview of multiphase flow modeling and fluid-structure interaction. It includes a mathematical formulation of multiphase flow, a classification of numerical methods, and a review of past research in this field. Detailed study of surface tension, FSI and dynamic contact angle are presented. Also, the detailed scope of the work is explained.

4.1 Scope of the Work

To develop a model for Fluid–Structure Interaction (FSI) by combining the Mode Superposition method and the Lagrangian Differencing Dynamics (LDD) method in two-way partitioned weak coupling or explicit coupling. In terms of computational efficiency, the LDD method is advantageous compared to most popular meshless approaches, such as SPH, MPS and FPM [107, 108, 109]. The LDD method achieves large time steps with lower computational costs while maintaining second-order accuracy. It is well-suited for complex transient problems since it has the advantage of directly working on the surface mesh as boundary conditions [110, 28, 93, 33]. Using the mode superposition method with LDD, structural deformation is calculated for the fluid load using precalculated mode shapes and natural frequencies from the modal analysis. This approach leads to stable, robust, and computationally efficient FSI simulations. The method enables fluid-induced structural deformation to be weakly coupled into the flow solver. The deformation is obtained by using direct integration. The flow particles and vertices of the structure are advected in Lagrangian coordinates. This results in Lagrangian–Lagrangian coupling in space, while there is weak or explicit coupling in time. This ensures a more accurate representation of the interaction between fluid and structure in ship and offshore hydrodynamics. The efficiency of the LDD and Mode Superposition methods, operating directly on surface meshes, may lead to practical and effective ship and offshore hydrodynamic simulations.

Further, the need for extending the original LDD framework to multiphase flows arises from its limitations when addressing scenarios where fluids of differing densities and viscosities interact. Although the LDD method has shown high effectiveness in modelling incompressible single-phase flows with large viscosity variations, multiphase flows introduce additional complexities such as capturing sharp interfaces and handling abrupt changes in flow field properties across these interfaces. For instance, a critical requirement in multiphase simulations is to maintain a stable interface with a sharp transition in density and pressure, as well as a robust management of high gradients in viscosity. Extending LDD to multiphase applications, enables it to address these challenges, maintaining both accuracy and stability even in the presence of complex fluid interactions.

4.2 Future Research

To develop a multiphase Lagrangian Differencing Dynamics (MP-LDD) approach, a novel enhancement of the Lagrangian Differencing Dynamics (LDD) method specifically designed for stable and accurate multiphase flow simulations is required. By incorporating a variable coefficient Laplacian, MP-LDD can achieve precise discretization of pressure and velocity fields, effectively addressing variations in density and viscosity, thereby enabling a more accurate representation of multiphase interactions. MP-LDD can employ

a unified single pressure and velocity equation applicable to both phases, in contrast to separate equations for each phase. Furthermore, a modified Position-Based Dynamics (PBD) framework can ensure the interface stability under varying density conditions. This framework is essential for simulating flows with high-density ratios and mitigating unintended mixing between immiscible fluids. Additionally, this can facilitate the management of pressure jumps across interfaces, enhancing the practicality of phase interactions while guaranteeing continuous acceleration and preventing void formation. These innovations will establish MP-LDD as a GPU-based, high-performance tool that provides efficient and accurate modeling capabilities for complex multiphase flows, highlighting its wide applicability across various multiphase scenarios. A novel multiphase Lagrangian Differencing Dynamics (MP-LDD), GPU based method will be developed to address specific challenges in multiphase flow simulation. The solver's meshless approach is ideal for precision spraying in printing and electronics, paint atomization through ultrasonic waves, underwater engineering with wave interactions, and environmental simulations like sediment transport and oil spills. It also addresses phase change in cooling systems and thermal processes in metal casting and additive manufacturing. By incorporating acoustic forces and droplet dynamics, the solver provides a powerful tool for simulating intricate multiphase flows across various industries. Additionally, a weak coupling approach to fluid-structure interaction will be introduced. The solver's objectives focus on ease of use, efficiency, scalability, and compatibility with complex multiphase scenarios. The core goals of MP-LDD are outlined in the sections below. These objectives demonstrate MP-LDD's commitment to meeting critical needs in computational fluid dynamics by offering an innovative and accessible approach to multiphase flow modeling.

4.2.1 Meshless Method

Unlike traditional grid-based approaches, MP-LDD is a meshless method. This eliminates the need for a predefined grid structure, enhancing the solver's flexibility in handling complex domain geometries. The meshless nature of MP-LDD is advantageous in scenarios where interface tracking is challenging, such as in high-density-ratio multiphase flows, since it allows particles to move freely without being constrained by grid boundaries.

4.2.2 GPU-Based Solver

The MP-LDD method leverages a GPU-based computational framework, allowing for significantly faster processing times. This parallel computing capability is essential for handling the high computational demands of multiphase simulations, particularly those involving complex interactions like Rayleigh-Taylor instabilities and fluid-solid interactions. GPU support also aids in reducing simulation time, making the method suitable for real-time or near-real-time applications in engineering.

4.2.3 Ease of Setup

A primary goal of MP-LDD is to streamline the setup process, making it accessible for researchers and engineers with varied expertise levels. By reducing the complexity of input parameters and optimizing initialization procedures, MP-LDD minimizes the time required to begin simulations. This simplicity allows users to focus more on analyzing results and less on complex setup configurations, improving workflow efficiency.

4.2.4 Scalability

MP-LDD is designed for easy scalability to large simulations. Its meshless nature and GPU-based acceleration allow it to handle a large number of particles without a significant compromise on performance. Scalability is further facilitated by the variable Laplacian framework in multiphase, which supports high density and viscosity ratios while maintaining interface sharpness and stability across extensive simulations.

4.2.5 Rapid Development Cycle

MP-LDD aims to provide a platform that allows for quick adjustments and testing, enabling rapid prototyping of new physical models and modifications. The straightforward nature of the Position-Based Fluids (PBF) approach in MP-LDD, combined with its stable and sharp interface, provides a development-friendly environment. This objective is particularly beneficial in research and development, where fast iteration is essential for testing new hypotheses or exploring novel applications.

4.2.6 Novel Applications

Our focus is on utilizing the innovative Multiphase Lagrangian Differencing Dynamics (MP-LDD) method to tackle challenging multiphase scenarios with fluid structure interaction.

- **Hydrogen Appplication:** Accurate modeling of bubble dynamics and phase interfaces plays a crucial role in hydrogen generation processes, such as water electrolysis and steam reforming. Additionally, the safe storage and efficient mobility of hydrogen rely on understanding multiphase flow phenomena, including gas-liquid interactions, surface tension effects, and dynamic wetting behavior.
- **Paintshop Processes:** In spray coating and painting applications, surface tension, fluid deformation, and contact angle dynamics are critical in ensuring uniform coating thickness and smooth finishes, especially on complex automotive and aircraft surfaces. In dip coating, objects are submerged in a liquid to form a uniform coating layer. The effects of dynamic wetting is to optimize coating thickness and uniformity. This is crucial for industries like automotive, electronics, and consumer goods. In dip Deformation Analysis, understanding fluid flow and deformation during dip coating in automotive paint shop processes is essential for achieving consistent finishes. Multiphase flow simulations with fluid-structure interactions (FSI) help analyze dip deformation.
- **Gearbox Oil Distribution:** The simulation of oil distribution in gearboxes involves violent multiphase flow, high-speed rotation, and fluid-structure interactions. Accurate modeling of such complex physical processes helps optimize lubrication performance and minimize wear in automotive and industrial applications.
- **Biofouling and Hydrophobic Surfaces:** Hydrophobic surface design is critical for anti-fouling coatings and self-cleaning surfaces. By analyzing fluid-solid interactions and dynamic boundary conditions, these surfaces enhance resistance to biofouling and ensure longevity in marine, medical, and industrial applications.

- **Droplet Formation and Injection:** Surface tension dynamics play a pivotal role in droplet formation. Also, in ultrasonic sound-driven and surface tension driven fluid injection systems. This is vital for applications in space and microgravity environments, where conventional fluid dynamics are altered. Movement of droplets using electric forces, magnetic forces and thermo capillary action.
- **Laser Bed Welding:** Multiphase flow simulations are essential in laser bed welding to model molten metal dynamics, phase changes, and surface tension effects. These simulations help optimize weld quality, reduce defects, and improve precision in advanced manufacturing processes.

References

[1] J. W. Cahn and J. E. Hilliard. "Free energy of a nonuniform system. I: Interfacial free energy". In: *The Journal of Chemical Physics* 28 (1958), pp. 258–267. DOI: https://doi.org/10.1063/1.1744102.

[2] C.W. Hirt and B.D. Nichols. "Volume of fluid (VOF) method for the dynamics of free boundaries". In: *Journal of Computational Physics* 39 (1981), pp. 201–225. DOI: https://doi.org/10.1016/0021-9991(81)90145-5.

[3] M. Sussman, P. Smereka, and S. Osher. "A Level Set approach for computing solutions to incompressible two-phase flow". In: *Journal of Computational Physics* 114.1 (1994), pp. 146–159. DOI: 10.1006/jcph.1994.1155.

[4] Grétar Tryggvason, R. Scardovelli, and S. Zaleski. *Direct numerical simulations of gas–liquid multiphase flows*. Cambridge University Press, 2011. DOI: https://doi.org/10.1017/CBO9780511975264.

[5] Maxime Theillard, Frédéric Gibou, and David Saintillan. "Sharp numerical simulation of incompressible two-phase flows". In: *Journal of Computational Physics* (2019). URL: www.elsevier.com/locate/jcp.

[6] J. J. Monaghan and A. Kocharyan. "SPH simulation of multiphase flow". In: *Computer Physics Communications* 87 (1995), pp. 225–235. DOI: 10.1016/0010-4655(94)00174-Z.

[7] Guangtao Duan et al. "Stable Multiphase Moving Particle Semi-implicit Method for Incompressible Interfacial Flow". In: (2017). DOI: https://doi.org/10.1016/j.cma.2017.01.002.

[8] C. Hirt, J. Cook, and T. Butler. "A Lagrangian method for calculating the dynamics of an incompressible fluid with free surface". In: *Journal of Computational Physics* 5.1 (1970), pp. 103–124.

[9] G. Ryskin and L. Leal. "Numerical solution of free-boundary problems in fluid mechanics. Part 1. the finite-difference technique". In: *Journal of Fluid Mechanics* 148 (1984), pp. 1–17.

[10] G. Ryskin and L. Leal. "Numerical solution of free-boundary problems in fluid mechanics. Part 2. buoyancy-driven motion of a gas bubble through a quiescent liquid". In: *Journal of Fluid Mechanics* 148 (1984), pp. 19–35.

[11] F. Zonta, A. Soldati, and M. Onorato. "Growth and spectra of gravity-capillary waves in countercurrent air/water turbulent flow". In: *Journal of Fluid Mechanics* 777 (2015), pp. 245–259.

[12] James Glimm. "Tracking of interfaces for fluid flow: Accurate methods for piecewise smooth problems". In: *Transonic, Shock, and Multidimensional Flows*. Academic Press, 1982, pp. 259–287.

[13] James Glimm and Oliver A. McBryan. "A computational model for interfaces". In: *Advances in Applied Mathematics* 6.4 (1985), pp. 422–435.

[14] H. S. Udaykumar et al. "Multiphase dynamics in arbitrary geometries on fixed cartesian grids". In: *Journal of Computational Physics* 137.2 (1997), pp. 366–405.

[15] R. Fedkiw et al. "A non-oscillatory Eulerian approach to interfaces in multimaterial flows (the ghost fluid method)". In: *Journal of Computational Physics* 152.2 (1999), pp. 457–492.

[16] Stéphane Popinet and Stéphane Zaleski. "A front-tracking algorithm for accurate representation of surface tension". In: *International Journal for Numerical Methods in Fluids* 30.6 (1999), pp. 775–793.

[17] Li Lee and Randall J. LeVeque. "An immersed interface method for incompressible Navier–Stokes equations". In: *SIAM Journal on Scientific Computing* 25.3 (2003), pp. 832–856.

[18] Dimitris Drikakis, Michael Frank, and Gavin Tabor. "Multiscale Computational Fluid Dynamics". In: *Energies* 12.17 (2019). ISSN: 1996-1073. DOI: 10.3390/en12173272. URL: https://www.mdpi.com/1996-1073/12/17/3272.

[19] J.U. Brackbill, D.B. Kothe, and C. Zemach. "A continuum method for modeling surface tension". In: *Journal of Computational Physics* 100.2 (1992), pp. 335–354.

[20] S.F. Kistler. *Hydrodynamics of wetting*. Ed. by J. C. Berg. Marcel Dekker, 1993, pp. 311–429.

[21] Robert L Hoffman. "A study of the advancing interface. I. Interface shape in liquid-gas systems". In: *Journal of Colloid and Interface Science* 50.2 (1975), pp. 228–241.

[22] Lawrence H Tanner. "The spreading of silicone oil drops on horizontal surfaces". In: *Journal of Physics D: Applied Physics* 12.9 (1979), p. 1473.

[23] Yulii D Shikhmurzaev. *Capillary flows with forming interfaces*. CRC Press, 2007.

[24] RG Cox. "The dynamics of the spreading of liquids on a solid surface. Part 1. Viscous flow". In: *Journal of Fluid Mechanics* 168 (1986), pp. 169–194.

[25] J. Göhl et al. "Dynamic wetting of droplet impingement: Theoretical and numerical modeling". In: *Physics of Fluids* 30.8 (2018), p. 082103.

[26] Kensuke Yokoi et al. "Numerical studies of the influence of the dynamic contact angle on a drop impacting on a dry surface". In: *Physics of Fluids* 21 (July 2009). DOI: 10.1063/1.3158468.

[27] Jonathan M. Ludwicki et al. "Is contact-line mobility a material parameter?" In: *NPJ Microgravity* 8 (2022). ISSN: 2373-8065. DOI: 10.1038/s41526-022-00190-y.

[28] M. Bašić et al. "Coupling of Non–Newtonian meshless flow with structural solvers". In: *Proceedings of the VII International Conference on Particle-Based Methods, PARTICLES*. Hamburg, Germany, 2021, 4–6 October. DOI: 10.23967/particles.2021.025.

[29] M. Paneer et al. "Elastic Behaviours of Linear Structure Using Modal Superposition and Lagrangian Differencing Dynamics". In: *Proceedings of the VIII International Conference on Particle-Based Methods PARTICLES 2023*. Milan, Italy.

[30] R. CoGroth et al. "Validation of High Fidelity Computational Methods for Aeronautical FSI Analyses". In: *Engineering Toward Green Aircraft—CAE Tools for Sustainable Mobility*. Vol. 92. Springer International Publishing, 2020, pp. 29–70.

[31] F. Debrabandere et al. "Fluid-Structure interaction using a Modal Approach". In: *J. Turbomach.* 134 (2012), p. 051043. DOI: 10.1115/1.4004859.

[32] Josip Bašić, Nastia Degiuli, and Dario Ban. "A class of renormalised meshless Laplacians for boundary value problems". In: *Journal of Computational Physics* 354 (2018), pp. 269–287. DOI: 10.1016/j.jcp.2017.11.003.

[33] J. Bašić et al. "Lagrangian differencing dynamics for incompressible flows". In: *J. Comput. Phys.* 462 (2022), p. 111198. DOI: 10.1016/j.jcp.2022.111198.

[34] J. Basic et al. "A renormalisation procedure for Lagrangian simulations of multiphase flows". In: *Comput. Fluids* 233 (2023), p. 105073. DOI: 10.1016/j.compfluid.2023.105073.

[35] Josip Bašić et al. "A Lagrangian Finite Difference Method for Sloshing: Simulations and Comparison with Experiments". In: *Proceedings of The 29th International Ocean and Polar Engineering Conference*. Honolulu, Hawaii, USA: International Society of Offshore and Polar Engineers, 2019.

[36] Josip Bašić, Nastia Degiuli, and Dario Ban. "Lagrangian differencing dynamics for incompressible flows". In: *Journal of Computational Physics* 429 (2021), p. 109821. DOI: 10.1016/j.jcp.2021.109821. URL: http://refhub.elsevier.com/S0266-352X(21)00295-0/h0020.

[37] Martina Bašić et al. "Coupling of Non-Newtonian Meshless Flow with Structural Solvers". In: *Proceedings of the VII International Conference on Particle-Based Methods (PARTICLES 2021)*. Online: Institute of Particle-Based Methods, 2021.

[38] Chong Peng et al. "A Lagrangian differencing dynamics method for granular flow modeling". In: *Journal of Computational Physics* 457 (2022), p. 111198. DOI: 10.1016/j.jcp.2022.111198.

[39] Manigandan Paneer et al. "Elastic Behaviours of Linear Structure Using Modal Superposition and Lagrangian Differencing Dynamics". In: *Proceedings of the VIII International Conference on Particle-Based Methods (PARTICLES 2023)*. Online: Institute of Particle-Based Methods, 2023.

[40] Manigandan Paneer et al. "Fluid Structure Interaction Using Modal Superposition and Lagrangian CFD". In: *Journal of Marine Science and Engineering* 12.2 (2024), p. 318. DOI: 10.3390/jmse12020318. URL: https://doi.org/10.3390/jmse12020318.

[41] Johannes C. Joubert, Daniel N. Wilke, and Patrick Pizette. "A Generalized Finite Difference Scheme for Multiphase Flow". In: *Mathematical and Computational Applications* 28.2 (2023). ISSN: 2297-8747. DOI: 10.3390/mca28020051. URL: https://www.mdpi.com/2297-8747/28/2/51.

[42] S. Osher and J.A. Sethian. "Fronts propagating with curvature-dependent speed: algorithms based on Hamilton-Jacobi formulations". In: *Journal of Computational Physics* 79 (1988), pp. 12–49. DOI: https://doi.org/10.1016/0021-9991(88)90002-2.

[43] S.O. Unverdi and G. Tryggvason. "A front-tracking method for viscous, incompressible, multi-fluid flows". In: *Journal of Computational Physics* 100 (1992), pp. 25–37. DOI: https://doi.org/10.1016/0021-9991(92)90307-K.

[44] E. Olsson and G. Kreiss. "A conservative level set method for two phase flow". In: *Journal of Computational Physics* 210 (2005), pp. 225–246. DOI: https://doi.org/10.1016/j.jcp.2005.04.007.

[45] K. Kamran, R. Rossi, and E. Oñate. "A locally extended finite element method for the simulation of multi-fluid flows using the Particle Level Set method". In: *Computer Methods in Applied Mechanics and Engineering* (2015). DOI: 10.1016/j.cma.2015.05.017.

[46] R. A. Gingold and J. J. Monaghan. "Smoothed particle hydrodynamics: Theory and application to non-spherical stars". In: *Monthly Notices of the Royal Astronomical Society* 181 (1977), pp. 375–389. DOI: https://doi.org/10.1093/mnras/181.3.375.

[47] L. B. Lucy. "A numerical approach to the testing of the fission hypothesis". In: *The Astronomical Journal* 82.6 (1977), pp. 1013–1024.

[48] S. Koshizuka and Y. Oka. "Moving-particle semi-implicit method for fragmentation of incompressible fluid". In: *Nuclear Science and Engineering* 123.3 (1996), pp. 421–434. DOI: 10.13182/NSE96-A24205.

[49] T. Belytschko, Y. Y. Lu, and L. Gu. "Element-free Galerkin methods". In: *International Journal for Numerical Methods in Engineering* 37.2 (1994), pp. 229–256. DOI: https://doi.org/10.1002/nme.1620370205. eprint: https://onlinelibrary.wiley.com/doi/pdf/10.1002/nme.1620370205. URL: https://onlinelibrary.wiley.com/doi/abs/10.1002/nme.1620370205.

[50] Eugenio Oñate Sergio Idelsohn Monica Mier-Torrecilla. "Multi-fluid flows with the Particle Finite Element Method". In: *Computer Methods in Applied Mechanics and Engineering* 198.33-36 (2009), pp. 2750–2767. DOI: 10.1016/j.cma.2009.03.004.

[51] J. J. Monaghan. "Smoothed particle hydrodynamics". In: *Annual Review of Astronomy and Astrophysics* 30 (1992), pp. 543–574. DOI: https://doi.org/10.1146/annurev.aa.30.090192.002551.

[52] J. P. Morris, P. J. Fox, and Y. Zhu. "Modeling low Reynolds number incompressible flows using SPH". In: *Journal of Computational Physics* 136.1 (1997), pp. 214–226.

[53] Benedict W. Ritchie and Peter A. Thomas. "Multiphase smoothed-particle hydrodynamics". In: *Monthly Notices of the Royal Astronomical Society* 323.3 (May 2001), pp. 743–756. ISSN: 0035-8711. DOI: 10.1046/j.1365-8711.2001.04268.x. eprint: https://academic.oup.com/mnras/article-pdf/323/3/743/3969896/323-3-743.pdf. URL: https://doi.org/10.1046/j.1365-8711.2001.04268.x.

[54] X.Y. Check Hu and N.A. Adams. "A multi-phase SPH method for macroscopic and mesoscopic flows". In: *Monthly Notices of the Royal Astronomical Society* 213.2 (2006), pp. 844–861. DOI: https://doi.org/10.1016/j.jcp.2005.09.001.

[55] N. Grenier et al. "An Hamiltonian interface SPH formulation for multi-fluid and free-surface flows". In: *Journal of Computational Physics* 228.22 (2009), pp. 8380–8393. DOI: https://doi.org/10.1016/j.jcp.2009.08.009.

[56] J. J. Monaghan et al. "A robust SPH algorithm for simulating immiscible multiphase flows". In: *Journal of Computational Physics* 231.4 (2012), pp. 345–360.

[57] M. Rezavand. "ISPH scheme for simulating multiphase flows with complex interfaces and high density ratios". In: *Journal of Computational Physics* 365.Issue Number (2018), pp. 106–123. DOI: https://doi.org/10.1016/j.camwa.2017.12.034.

[58] Massoud Rezavand, Chi Zhang, and Xiangyu Hu. "A weakly compressible SPH method for violent multi-phase flows with high density ratio". In: *Journal of Computational Physics* Volume Number.Issue Number (2019). DOI: https://doi.org/10.1016/j.jcp.2020.110028.

[59] Y. Shimizu. "Enhanced multiphase ISPH-based method for accurate modeling of oil spill". In: *Journal of Computational Physics* 400.Issue Number (2020), p. 104129. DOI: https://doi.org/10.1080/21664250.2020.1815362.

[60] M. Olejnik and J. Pozorski. "A robust method for wetting phenomena within smoothed particle hydrodynamics". In: *Flow, Turbulence and Combustion* 104.1 (2020), pp. 115–137. DOI: https://doi.org/10.1007/s10494-019-00048-6.

[61] R. Vacondio et al. "Grand challenges for smoothed particle hydrodynamics numerical schemes". In: *Computational Particle Mechanics* 8.4 (2021), pp. 575–588. DOI: 10.1007/s40571-020-00354-1. URL: https://link.springer.com/article/10.1007/s40571-020-00354-1.

[62] Chi Zhang, Yujie Zhu, and Xiangyu Hu. "A multi-resolution SPH framework: Application to multi-phase fluid-structure interactions". In: *physics.flu-dyn* (2022), pp. 5082–5101. DOI: https://doi.org/10.48550/arXiv.2205.00707. eprint: 2205.00707.

[63] Guangtao Duan et al. "An accurate and stable multiphase moving particle semi-implicit method based on a corrective matrix for all particle interaction models". In: *International Journal for Numerical Methods in Engineering* 115.10 (2018), pp. 1287–1314. DOI: https://doi.org/10.1002/nme.5844. eprint: https://onlinelibrary.wiley.com/doi/pdf/10.1002/nme.5844. URL: https://onlinelibrary.wiley.com/doi/abs/10.1002/nme.5844.

[64] Ronald P. Fedkiw et al. "A non-oscillatory Eulerian approach to interfaces in multimaterial flows (the ghost fluid method)". In: *Journal of Computational Physics* 152.2 (1999), pp. 457–492. DOI: https://doi.org/10.1006/jcph.1999.6236.

[65] D.M. Anderson, G.B. McFadden, and A.A. Wheeler. "Diffuse-interface methods in fluid mechanics". In: *Annual Review of Fluid Mechanics* 30.1 (1998), pp. 139–165. DOI: https://doi.org/10.1146/annurev.fluid.30.1.139.

[66] X. Shan and H. Chen. "Lattice Boltzmann model for simulating flows with multiple phases and components". In: *Physical Review E* 47.3 (1993), pp. 1815–1819. DOI: https://doi.org/10.1103/PhysRevE.47.1815.

[67] J.P. Morris. "Modeling low Reynolds number incompressible flows using smoothed particle hydrodynamics". In: *International Journal for Numerical Methods in Fluids* 33.3 (2000), pp. 333–353.

[68] Thomas Young. "An essay on the cohesion of fluids". In: *Philosophical Transactions of the Royal Society of London* 95 (1805), pp. 65–87.

[69] Pierre-Simon Laplace. *Mécanique Céleste*. Vol. 4. Paris: Courcier, 1806.

[70] William D. Harkins and Herbert F. Jordan. "A method for determining surface tension and contact angle from the profile of a sessile drop". In: *Journal of the American Chemical Society* 52.5 (1930), pp. 1751–1772.

[71] Terence D. Blake and John M. Haynes. "Kinetics of liquid/liquid displacement". In: *Journal of Colloid and Interface Science* 30.3 (1969), pp. 421–423. DOI: 10.1016/0021-9797(69)90411-1.

[72] Jean-François Joanny and Pierre-Gilles de Gennes. "A model for contact angle hysteresis". In: *Journal of Chemical Physics* 81.11 (1984), pp. 5527–5530.

[73] Charles W. Extrand and Alan G. Shapiro. "Apparent contact angles and retention of liquids on horizontal surfaces". In: *Journal of Colloid and Interface Science* 170.2 (1995), pp. 515–521.

[74] OV Voinov. "Hydrodynamics of wetting". In: *Fluid Dynamics* 11.5 (1976), pp. 714–721.

[75] Y.D. Shikhmurzaev. "Moving contact lines in liquid/liquid/solid systems". In: *Journal of Fluid Mechanics* 334 (1997), pp. 211–249. DOI: 10.1017/S0022112096004350.

[76] D. V. Nichita, R. Sander, and H. Ghassemi. "Dynamic receding contact angle model for multiphase flow simulations". In: *International Journal of Multiphase Flow* 36 (2010), pp. 935–947. DOI: 10.1016/j.ijmultiphaseflow.2010.06.007.

[77] J. Göhl et al. "An immersed boundary based dynamic contact angle framework for handling complex surfaces of mixed wettabilities". In: *International Journal of Multiphase Flow* 109 (2018), pp. 164–177.

[78] Jacco H. Snoeijer and Bruno Andreotti. "Moving contact lines: Scales, regimes, and dynamical transitions". In: *Annual Review of Fluid Mechanics* 45 (2013), pp. 269–292.

[79] L. Huang et al. "Fluid–structure interaction of a large ice sheet in waves". In: *Ocean. Eng. Ser.* 182 (2019), pp. 102–111. DOI: 10.1016/j.oceaneng.2019.03.001.

[80] F. Danielsen et al. "The Asian tsunami: A protective role for coastal vegetation". In: *Science* 310 (2005), p. 643. DOI: 10.1126/science.1117158.

[81] W. Zhou, Z. Wu, and L. Mevel. "Vibration-based damage detection to the composite tank filled with fluid". In: *Struct. Health Monit.* 9 (2010), pp. 433–445. DOI: 10.1177/1475921710365885.

[82] M.A. Chella, A. Tørum, and D. Myrhaug. "An overview of wave impact forces on offshore wind turbine substructures". In: *Energy Procedia* 20 (2012), pp. 217–226. DOI: 10.1016/j.egypro.2012.03.026.

[83] L. Liang et al. "Hydrodynamic performance optimization of marine propellers based on fluid–structure coupling". In: *Brodogradnja* 74 (2023), pp. 145–164. DOI: 10.21278/brod74310.

[84] Z. Zhang et al. "On the propeller wake evolution using large eddy simulations and physics-informed space-time decomposition". In: *Brodogradnja* 75 (2024), p. 75102. DOI: 10.21278/brod75102.

[85] J.J. Jensen. *Load and Global Response of Ships*. Amsterdam, The Netherlands: Elsevier, 2001, pp. 268–271. URL: https://www.sciencedirect.com/bookseries/elsevier-ocean-engineering-series/vol/4/suppl/C.

[86] A. Kwang-Jun Paik et al. "Strongly coupled fluid–structure interaction method for structural loads on surface ships". In: *Ocean. Eng.* 36 (2009), pp. 1346–1357. DOI: 10.1016/j.oceaneng.2009.07.006.

[87] J. Hron and S. Turek. "A monolithic FEM/multigrid solver for an ALE formulation of fluid–structure interaction with applications in biomechanics". In: *Fluid–Struct. Interact.* 53 (2006), pp. 146–170. DOI: 10.1016/j.fsi.2006.02.003.

[88] J. Hron and S. Turek. "A monolithic FEM solver for an ALE formulation of fluid–structure interaction with configuration for numerical benchmarking". In: *Proceedings of the European Conference on Computational Fluid Dynamics*. Egmond aan Zee, The Netherlands, 2006, 5–8 September.

[89] S. Rugonyi and K.J. Bathe. "On finite element analysis of fluid flows fully coupled with structural interactions". In: *CMES* 2 (2001), pp. 195–212. DOI: https://doi.org/10.3970/cmes.2001.002.195.

[90] J. Degroote et al. "Partitioned solution of an unsteady adjoint for strongly coupled fluid–structure interactions and application to parameter identification of a one-dimensional problem". In: *Struct. Multidiscip. Optim.* 47 (2013), pp. 77–94. DOI: 10.1007/s00158-012-0824-4.

[91] J. Degroote et al. "Coupling techniques for partitioned fluid–structure interaction simulations with black-box solvers". In: *Proceedings of the 10th MpCCI User Forum*. Sankt Augustin, Germany, 2009, 17–18 February. URL: https://lib.ugent.be/catalog/pug01:940479.

[92] W.Z. Lim et al. "Partitioned methods in computational modelling on fluid–structure interactions of concrete gravity-dam". In: *Comput. Informat. Sci.* 6 (2013), p. 154. DOI: 10.1007/s42184-018-0007-4.

[93] J. Bašić, N. Degiuli, and Š. Malenica. "Insight into Hydrodynamic Damping of a Segmented Barge Using Numerical Free-Decay Tests". In: *J. Mar. Sci. Eng.* 11 (2023), p. 581. DOI: 10.3390/jmse11020581.

[94] S. Seng, J.J. Jensen, and Š. Malenica. "Global hydroelastic model for springing and whipping based on a free-surface CFD code (OpenFOAM)". In: *Int. J. Nav. Archit. Ocean Eng.* 6 (2014), pp. 1024–1040. DOI: 10.1017/S1657777414000332.

[95] M. Morishita et al. "Enhanced prediction of global ship response using a new hybrid numerical method based on a computational fluid dynamics–structural dynamics coupled approach". In: *J. Marine Sci. Technol.* 23 (2018), pp. 1–15. DOI: 10.1007/s00773-018-0536-3.

[96] Z. Tuković et al. "OpenFOAM Finite Volume Solver for Fluid-Solid Interaction". In: *Trans. Famena* 42.3 (2018), pp. 1–31. DOI: 10.21278/TOF.42301.

[97] E. Schillaci et al. "Numerical simulation of fluid structure interaction in free-surface flows: The WEC case". In: *J. Phys. Conf. Ser.* 2116 (2021), p. 012122. DOI: 10.1088/1742-6596/2116/1/012122.

[98] G. Fourey et al. "Violent fluid–structure interaction simulations using a coupled SPH/FEM method". In: *IOP Conf. Ser. Mater. Sci. Eng.* Vol. 10. 2010, p. 012041. DOI: 10.1088/1757-899X/10/1/012041.

[99] Q. Yang, V. Jones, and L. McCue. "Free-surface flow interactions with deformable structures using an SPH–FEM model". In: *Ocean Eng.* 55 (2012), pp. 136–147. DOI: 10.1016/j.oceaneng.2012.06.031.

[100] J. Nunez-Ramirez et al. "A partitioned approach for the coupling of SPH and FE methods for transient nonlinear FSI problems with incompatible time-steps". In: *Int. J. Numer. Methods Eng.* 109 (2017), pp. 1391–1417. DOI: 10.1002/nme.5331.

[101] K. Wu, D. Yang, and N. Wright. "A coupled SPH-dem model for fluid–structure interaction problems with free-surface flow and structural failure". In: *J. Comput. Struct.* 177 (2016), pp. 141–161. DOI: 10.1016/j.compstruc.2016.08.012.

[102] A.M.A. Nasar et al. "Flexible slender body fluid interaction: Vector-based discrete element method with Eulerian smoothed particle hydrodynamics". In: *Comput. Fluids* 179 (2019), pp. 563–578. DOI: 10.1016/j.compfluid.2018.11.024.

[103] O. Joseph and D. Rogers Benedict. "A fluid–structure interaction model for free-surface flows and flexible structures using smoothed particle hydrodynamics on a GPU". In: *J. Fluids Struct.* 104 (2021), p. 103312.

[104] J. Degroote. "Partitioned simulation of fluid–structure interaction". In: *Arch. Comput. Methods Eng.* 20 (2013), pp. 185–238. DOI: 10.1007/s11831-013-9085-5.

[105] K.Z. Sun et al. "Numerical analysis of violent hydroelastic problems based on a mixed MPS—mode superposition method". In: *Ocean. Eng.* 179 (2019), pp. 285–297. DOI: 10.1016/j.oceaneng.2019.03.032.

[106] J.W. Banks et al. "A stable partitioned FSI algorithm for rigid bodies and incompressible flow. Part I: Model problem analysis". In: *J. Comput. Phys.* 343 (2017), pp. 432–468. DOI: 10.1016/j.jcp.2017.01.015.

[107] S. Tiwari and J. Kuhnert. "Finite pointset method based on the projection method for simulations of the incompressible Navier–Stokes equations". In: *Meshfree Methods for Partial Differential Equations*. Springer, 2003, pp. 373–387.

[108] C. Drumm et al. "Finite pointset method for simulation of the liquid–liquid flow field in an extractor". In: *Comput. Chem. Eng.* 32 (2008), pp. 2946–2957. DOI: 10.1016/j.compchemeng.2008.03.009.

[109] E. Onate, F. Perazzo, and J. Miquel. "A finite point method for elasticity problems". In: *Comput. Struct.* 79 (2001), pp. 2151–2163. DOI: 10.1016/S0045-7949(01)00067-0.

[110] C. Peng et al. "A Lagrangian differencing dynamics method for granular flow modeling". In: *J. Comput. Geotech.* 137 (2021), p. 104297. DOI: 10.1016/j.compgeo.2021.104297.

List of Symbols and Abbreviations

β, α	Rayleigh constants
$\dot{\boldsymbol{y}}_t$	Velocity of current time step
$\dot{\boldsymbol{y}}_{t-1}$	Velocity of previous time step
$\boldsymbol{\Phi}$	Mass normalized modal vector
$\boldsymbol{C}$	Damping matrix
$\boldsymbol{f}(t)$	Applied forces over time
$\boldsymbol{K}$	Stiffness matrix
$\boldsymbol{M}$	Mass-normalized matrix
$\boldsymbol{u}$	Column vector corresponds to the degree of freedom
$\boldsymbol{y}_t$	Displacement of current time step
$\boldsymbol{y}_{t-1}$	Displacement of previous time step
$\delta(\phi)$	Dirac delta function
γ_{lg}	Liquid-gas surface tension
γ_{sg}	Solid-gas surface energy
γ_{sl}	Solid-liquid surface tension
κ	Curvature of the interface
λ	Slip length
$\mathbf{F}_s$	Surface tension force per unit volume
$\mathbf{g}$	Acceleration due to gravity
$\mathbf{n}$	Unit normal vector to the interface
$\mathbf{r}'$	Distance vector of the center point
$\mathbf{r}$	Distance vector of the neighbour point
$\mathbf{u}$	Velocity
$\mathbf{u}_0$	Radial velocity
$\mathbf{u}_{cl}$	Contact line velocity
μ	Dynamic viscosity
∇	Vector of partial derivative operator
$\nabla \cdot \mathbf{u}$	Velocity divergence

$\nabla \mathbf{u}$	Velocity gradient
∇H	Gradient of Heaviside function
∇p	Pressure gradient
$\nabla^2 \mathbf{u}$	Velocity Laplacian
ν	Kinematic viscosity
ω, ω_n	Natural Frequency
Ω	Domain around the interface
ϕ	Phase indicator
ρ	Density
σ	Surface tension coefficient
θ	Contact angle
θ_A	Advancing contact angle
θ_D	Dynamic contact angle
θ_E	Equilibrium contact angle
θ_R	Receding contact angle
θ_{app}	Apparent contact angle
θ_{mda}	Maximum dynamic advancing angle
θ_{mdr}	Maximum dynamic receding angle
ζ	Damping ratio
a_1, a_2	Fitted parameters
Ca	Capillary number
D/Dt	Material derivative
dt	Time step
$g(\theta)$	Integral function or g-function
$H(\phi)$	Heaviside function
k_a	Material dependent contacts for advancing
k_r	Material dependent contacts for receding
L	Apparent length
M	Mobility parameter

p Pressure

t Time

W Weighting function

$W(\mathbf{r} - \mathbf{r}')$ Smoothing kernel

$\partial/\partial t$ Partial derivative with time

BEM Boundary Element Method

BiCGSTAB Bi-Conjugate Gradient Stabilized Method

CFD Computational Fluid Dynamics

CFPI Complementary Function and Particular Integral

CPU Central Processing Unit

CSF Continuum Surface Force

DCA Dynamic Contact Angle

DEM Discrete Element Method

DES Detached Eddy Simulation

DIM Diffuse Interface Model

DOF Degree Of Freedom

DPD Dissipative Particle Dynamics

EFG Element-Free Galerkin

FDM Finite Difference Method

FEM Finite Element Method

FPM Finite Pointset Method

FSI Fluid-Structure Interaction

FVM Finite Volume Method

GFDM Generalized Finite Difference Method

GFM Ghost Fluid Method

GPU Graphics Processing Unit

IBM Immersed Boundary Method

ISPH Incompressible Smoothed Particle Hydrodynamic

LBM Lattice Boltzmann Method

LDD Lagrangian Differencing Dynamics

MAC Marker-and-Cell Method

MD Molecular Dynamic

MDOF Multi Degree Of Freedom

MLS Moving Least Square

MMPS Multiphase Moving Particle Semi-Implicit

MMPS-CA Multiphase Moving Particle Semi-Implicit - Continuous Acceleration

MMPS-HD Multiphase Moving Particle Semi-Implicit - Harmonic Density

MP-LDD Multiphase Lagrangian Differencing Dynamics

MPS Moving Particle Semi-Implicit

NVH Noise-Vibration-Harshness

ODE Ordinary Differential Equation

PBD Particle based Dynamics

PDE Partial Differential Equation

PDE Partial Differential Equations

PFEM Particle Finite Element Method

PLIC Piecewise Linear Interface Calculation

PLS Particle Level Set

PPE Pressure Poisson Equation

RANS Reynolds-averaged Navier–Stokes equation

SCSF Smoothed Continuum Surface Force

SDOF Single Degree Of Freedom

SPH Smoothed Particle Hydrodynamics

SSF Sharp Surface Force

URANS Unsteady Reynolds-averaged Navier–Stokes equation

VOF Volume of Fluid

XFEM Extended Finite Element Method

Abstract

Multiphase flow simulations are inherently complex due to the intricate interactions between different phases, especially when there are significant density and viscosity contrasts. These complexities often create challenges in accurately capturing sharp interfaces and managing pressure jumps across phases, which can lead to numerical instability. One of the main challenges in multiphase flow modeling is the accurate representation of phase interfaces. It is crucial to capture the movement, deformation, and interaction of phase boundaries to predict multiphase flow behavior accurately. Traditional grid-based methods frequently struggle to maintain sharp and stable interfaces, particularly in systems with high-density and high-viscosity variations. Techniques such as the Level Set and Volume of Fluid methods are commonly employed for interface tracking; however, they require complex algorithms to ensure numerical stability and avoid interface smearing. In addition to interface dynamics, surface tension forces significantly influence multiphase flows, especially in microscale systems where interfacial forces dominate inertial forces. Surface tension affects behaviors such as droplet coalescence, breakup, and spreading. Furthermore, dynamic contact angles, which describe the interactions between fluid phases and solid surfaces, introduce an additional layer of complexity to multiphase flow modeling. These angles can vary with flow conditions, impacting capillary-driven flows and surface wettability. Due to these complexities, multiphase flows can exhibit a wide range of behaviors, from stable stratified flows to highly chaotic and turbulent regimes. Thus, effectively modeling multiphase flows presents not only a significant scientific challenge but also a critical need for optimizing industrial applications, ensuring environmental safety, and advancing scientific research.

This paper provides an overview of multiphase flow modeling and fluid-structure interaction. It includes a mathematical formulation of multiphase flow and a classification of numerical methods, along with a review of past research in this field. Moreover, a novel multiphase, GPU-based solver will be developed, incorporating surface tension effects, dynamic contact angles, and phase change phenomena. Additionally, a weak coupling approach to fluid-structure interaction will be introduced.

Keywords: Multiphase, Pressure jump, Interface, Surface tension, Wettability and Dynamic contact angle